

1 **Authors response to reviewer's comments: Keys et al. BG-2017-510**

2

3 Dear authors,

4 Thank you for submitting a revised version of your manuscript. One of the original reviewers has  
5 examined it and considers that most comments and suggestions have been dealt with adequately.  
6 However, this reviewer lists numerous issues that still require attention before publication can be  
7 recommended. I also include below several points that need to be considered. Some of them are  
8 important, in particular those that concern 1) discussion of the implications of not having nutrient  
9 data, 2) interpretation of potential existence of feedback mechanisms, 3) comparison of properties  
10 between initial and final sampling date and 4) explanation of the antagonistic effect between high  
11 pCO<sub>2</sub> and warm temperature.

12 I now invite you to address these comments in a revised version of your manuscript.

13 Thank you for submitting your work to Biogeosciences.

14

15 Best regards,

16 Emilio Marañón

17

18 Editorial comments on BG-2017-510

19

20 - As indicated by reviewer 1, the Discussion must consider the implications of the lack of information  
21 on nutrient concentration. The text should explicitly mention that differences in nutrient availability  
22 may have contributed to observed differences between control and high temperature and high CO<sub>2</sub>  
23 treatments. The whole experiment rests on the assumption that initial nutrient concentrations were  
24 the same in every experimental bottle, but this assumption has not been verified. Assuming this was  
25 the case, and to the extent that differences in biomass were observed between treatments,  
26 differences in nutrient concentration must have arisen as well during the experiment.

27

28 **Response:** The text now explicitly mentions that differences in nutrient availability may have  
29 contributed to observed differences between control and high temperature and high CO<sub>2</sub>  
30 treatments (see Lines 445-447).

31

32 - Title must be changed to make it clear that what is being studied is a bloom induced experimentally  
33 in vitro.

34 **Response:** The title has been changed as suggested.

35

36 - Abstract line First sentence should clarify that the article deals with an experimentally induced  
37 bloom in vitro.

38 **Response:** The first sentence in the abstract has been changed to indicate that the article deals with  
39 an experimentally induced bloom in vitro.

40

41 - In the Abstract, and throughout the manuscript, changes in properties as a result of experimental  
42 treatments must be described in terms of the difference between treatment and control, not  
43 between treatment and initial value. For instance, lines 16-17 read: 'total phytoplankton biomass  
44 was significantly increased by elevated pCO<sub>2</sub> (20-fold) and (...) biomass also increased under

45 elevated temperature (15-fold)'. This passage suggests that high pCO<sub>2</sub> and warm temperature  
46 induced very large increases in biomass, when in fact those increases (20- and 15-fold) refer to the  
47 difference between final and initial values. Given that biomass increased also in the control bottles,  
48 the relevant comparison is between treatments and control. The same problem applies to the later  
49 reference to the 30-fold increase in *Prorocentrum cordatum*.

50 **Response:** *The manuscript has been modified to reflect differences between treatments rather than*  
51 *differences within treatments over time.*

52

53 Line 19 Add 'and in the control': 'Throughout the experiment in all treatments and in the control...'

54 **Response:** The sentence has been modified as suggested.

55

56 Lines 107-109 Note that pre-screening through 200-um mesh removes only the mesozooplankton.  
57 The microzooplankton (quantitatively more relevant, in terms of grazing pressure) are still present in  
58 the experimental bottles (see comment 2 by reviewer 2).

59 **Response:** *The sentence has been modified as suggested.*

60

61 - The assessment of chl-a-specific productivity is based on an indirect method (FRRF), which, as the  
62 authors acknowledge, is based on numerous untested assumptions. In addition, FRRF measurements  
63 were conducted on a single occasion in an experiment that lasted >30 days. This represents a tenuous  
64 base to make a major conclusion of the observation that the combined high pCO<sub>2</sub> and high  
65 temperature treatment causes no change in chl-a-normalised productivity.

66

67 **Response:** *We have now clearly pointed out that the measurements were only made at the end of*  
68 *the experiment and that robust conclusions cannot be made on this information alone.*

69

70 - Related to the point above, and as mentioned also by reviewer 1, the lack of effect of the  
71 combined high pCO<sub>2</sub> and high temperature treatment upon productivity is by no means an  
72 instance of negative feedback (as stated at the end of the Abstract and in the Discussion). In the  
73 context of CO<sub>2</sub>-induced climate change, an example of negative feedback would be an increase in  
74 marine productivity, which would contribute to counterbalance the original disturbance (higher  
75 pCO<sub>2</sub>). If, as a result of climate change, productivity decreases, then a positive feedback would be  
76 occurring. But if the environmental changes considered (in this case, temperature and pCO<sub>2</sub>  
77 combined) cause no effect on productivity, there is no feedback to speak of.

78

79 **Response:** *We have modified negative feedback to 'no feedback' (see lines 593 & 603-604).*

80

81 Lines 477-478 Many species have optimum temperatures higher than 20°C (Boyd et al. 2013  
82 PlosOne, Chen 2015 J Plankton Res)

83

84 **Response:** *This has now been stated (see lines 436-438).*

85

86 Lines 498-499 The logic behind this sentence is unclear: 'This may explain the lower PBm in the  
87 combined treatment compared to elevated pCO<sub>2</sub> and temperature individually'. If dinoflagellates

88 have weaker CCMs compared to diatoms, how does that explain the fact that at the end of the  
89 experiment PBm is smaller in the high CO<sub>2</sub> treatment, where DIC is more abundant? How can you  
90 connect a bulk property (PBm) with the abundance of dinoflagellates, which contribute a minor  
91 fraction (<20%) of all phytoplankton? And how can you explain the effect of temperature? The  
92 explanations of the antagonistic effect of temperature and pCO<sub>2</sub> on phytoplankton biomass and  
93 photosynthesis are confusing. This antagonistic effect is quite puzzling and, without trying to put  
94 forward speculative mechanisms, the authors might just acknowledge that additional studies are  
95 required to figure this out.

96 **Response:** This paragraph has now been edited to reflect your comments and make our assertions  
97 clearer.

98

99 Lines 493-494 Such high pH values denote strong consumption of DIC which is associated with  
100 nutrient depletion – hence slow growth rates likely result from nutrient limitation

101

102 **Response:** We have now acknowledged the role of nutrients in this sentence.

103

104 Line 560 Again, the sign of the potential feedback mechanism is wrong. If high CO<sub>2</sub> leads to higher  
105 photosynthesis and more CO<sub>2</sub> uptake by the ocean, this represents a negative feedback, not a  
106 positive one. It is a negative feedback because the outcome contributes to counterbalance or  
107 neutralize the original disturbance (hence it is a stabilising mechanism).

108

109 **Response:** We have now corrected this statement to ‘negative feedback’.

110

111 Line 581 There is no reduction, if productivity in the combined high CO<sub>2</sub> and warm temperature  
112 treatment was the same as in the control.

113 **Response:** This has now been stated (see lines 603-604).

114

115 Figure 3, Table 1, also section 3.4. The POC:PON ratio cannot have units of mg m<sup>-3</sup>. This ratio should  
116 be computed with molar concentrations, so that its units would be molC:molN.

117 **Response:** POC:PON has now been computed with molar concentrations and all associated sections,  
118 table and figures have been updated.

119

120 Anonymous reviewer:

121 1) While limited resources or time are an understandable reason why some data may not be  
122 available, you still have to discuss the scientific implications. For instance, what is the potential  
123 error/uncertainty and would it affect your conclusions.

124 **Response:** This has now been discussed

125

126 2) Phaeocystis was dominating the community towards the end of the experiment at high CO<sub>2</sub>,  
127 which nanophytoplankton group was dominating at elevated temperatures? In this respect, it  
128 appears a much more interesting/pressing question why phytoplankton biomass decreased in the  
129 control and combined treatment towards the end (while the two others continued on their  
130 trajectory) at nutrient replete conditions. Which direct or indirect effects could be responsible

131 (grazing)?

132

133 **Response:** Nanophytoplankton were enumerated by flow cytometry and it was not possible to  
134 discern the species, except for *Phaeocystis* spp., from this. A statement has been added to qualify  
135 this (see lines 357-358) and differences in nanophytoplankton size classes between treatments were  
136 previously highlighted in the results section.

137

138 3) L345: A bracket seems to be missing.

139 **Response:** Now corrected.

140

141 4) L362: 'weilessii' should be in lower case

142 **Response:** Now corrected, although we have maintained the spelling as 'wailesii' as per the  
143 literature and text books.

144

145 5) L414-422: What is a 'variability in the C acquisition strategy', how would it be different to other  
146 species and where is the reference? Also, it appears not so much a community shift towards  
147 *Phaeocystis*/nanophytoplankton at high CO<sub>2</sub>/high temperature but a switch towards a more diverse  
148 community in the control/combined treatments (also see my comment #1 and 2).

149

150 **Response:** We have now re-written this section of the paragraph

151

152 6) L430: It should read 'Chl a ratios'

153

154 **Response:** This has been corrected.

155

156 7) L430: Chlorophyll a is rather constant in comparison to the changes in biomass between day 25  
157 and 36. Also, there is no data on an overall biomass decrease between T25 and T27.

158 **Response:** The data clearly shows a biomass decrease between T25 and T27

159

160 8) L433: Is there any evidence from the literature that Chl a to biomass/carbon ratios in these groups  
161 could explain your findings?

162 **Response:** We have now referenced this statement.

163

164 9) L439: There was no higher community biomass at elevated pCO<sub>2</sub> in the Riebesell et al. (2007)  
165 study. On this note the Delille et al. 2005 paper is on the same experiment. Furthermore, there was  
166 no significant CO<sub>2</sub> effects on POC/PON in Riebesell et al. 2007 (L455). Finally, I am not aware of  
167 reports of P<sub>bmax</sub> in the Riebesell et al. 2009 study.

168

169 **Response:** The reference to high biomass in Riebesell et al. (2007) has been removed (see line 468).

170

171 10) L478: There are definitely species which grow faster beyond temperatures of 20 degrees Celsius.

172 **Response:** This sentence has now been changed.

173

174 11) L564: The establishment of hypoxic zones would require eutrophic conditions.

175 **Response:** This has been clarified on lines 598-599.

176

177 12) L569: If there is no effect on P<sub>bmax</sub> in the future treatment of combined temperature and CO<sub>2</sub>  
178 increase in comparison to the control treatment which represents current conditions, then there are  
179 also no feedbacks on atmospheric CO<sub>2</sub>.

180 **Response:** This has been corrected.

181

182 13) In the supplement, rather than showing absolute PAR measured in the incubation, you could  
183 consider showing the ratio to that in air.

184 **Response:** This figure has now been revised.

185

186 14) Last but not least, you did not answer my question of how the flow cytometer was calibrated in  
187 terms of size measurements.

188 **Response:** The calibration of the flow cytometry method has now been added to 'supplementary  
189 material'.

190

191

192 **Effects of elevated CO<sub>2</sub> and temperature on phytoplankton community**  
193 **biomass, species composition and photosynthesis during an**  
194 **experimentally induced -autumn bloom in the Western English**  
195 **Channel**

196 Matthew Keys<sup>1,2</sup>, Gavin Tilstone<sup>1\*</sup>, Helen S. Findlay<sup>1</sup>, Claire E. Widdicombe<sup>1</sup> and Tracy Lawson<sup>2</sup>.

197 <sup>1</sup> Plymouth Marine Laboratory, Prospect Place, The Hoe, Plymouth, PL1 3DH, UK.

198 <sup>2</sup> University of Essex, Wivenhoe Park, Colchester, CO4 3SQ, UK.

199 *Correspondence to:* G. Tilstone (ghti@pml.ac.uk)

200

201 **Abstract**

202 The combined effects of elevated pCO<sub>2</sub> and temperature were investigated during an  
203 experimentally induced autumn phytoplankton bloom *in vitro* ~~in~~ sampled from the Western  
204 English Channel (WEC). A full factorial 36-day microcosm experiment was conducted under

205 year 2100 predicted temperature (+ 4.5 °C) and pCO<sub>2</sub> levels (800 µatm). ~~The starting~~  
206 ~~phytoplankton community biomass was 110.2 (± 5.7 sd) mg carbon (C) m<sup>-3</sup> and was dominated~~  
207 ~~by dinoflagellates (~50 %) with smaller contributions from nanophytoplankton (~13 %),~~  
208 ~~cryptophytes (~11 %) and diatoms (~9 %).~~ Over the experimental period total phytoplankton  
209 biomass was significantly ~~increased~~ influenced by elevated pCO<sub>2</sub>. ~~(20-fold) and a~~ At the end of  
210 the experiment, biomass increased 6.5-fold under elevated pCO<sub>2</sub> and 4.6-fold also increased  
211 under elevated temperature relative to the ambient control (15-fold). By contrast, the combined  
212 influence of elevated pCO<sub>2</sub> and temperature had little effect on biomass relative to the control.  
213 Throughout the experiment in all treatments and in the control, the phytoplankton community  
214 structure shifted from dinoflagellates to nanophytoplankton. At the end of the experiment,  
215 under elevated pCO<sub>2</sub> nanophytoplankton contributed 90% of community biomass and was  
216 dominated by *Phaeocystis* spp.. Under elevated temperature, nanophytoplankton comprised  
217 85% of the community biomass and was dominated by smaller nano-flagellates. In the control,  
218 larger nano-flagellates dominated whilst the smallest nanophytoplankton contribution was  
219 observed under combined elevated pCO<sub>2</sub> and temperature (~40 %). Under elevated pCO<sub>2</sub>,  
220 temperature and in the control, there was a significant decrease in dinoflagellate biomass.  
221 Under the combined effects of elevated pCO<sub>2</sub> and temperature, dinoflagellate biomass increased  
222 almost doubled from the starting value and there was a 30-fold increase in and was dominated  
223 by the harmful algal bloom (HAB) species, *Prorocentrum cordatum*. At the end of experiment,  
224 Chlorophyll a (Chl *a*) normalised maximum photosynthetic rates (P<sup>B<sub>m</sub></sup>) increased > 6-fold under  
225 elevated pCO<sub>2</sub> and > 3-fold under elevated temperature while no effect on P<sup>B<sub>m</sub></sup> was observed  
226 when pCO<sub>2</sub> and temperature were elevated simultaneously. The results suggest that future  
227 increases in temperature and pCO<sub>2</sub> simultaneously do not appear to influence coastal  
228 phytoplankton productivity but significantly influence community composition during autumn  
229 in the WEC. ~~which would have a negative feedback on atmospheric CO<sub>2</sub>.~~

## 230 1. Introduction

231 Oceanic concentration of CO<sub>2</sub> has increased by ~42% over pre-industrial levels, with a  
232 continuing annual increase of ~0.4%. Current CO<sub>2</sub> level has reached ~400 µatm and has been  
233 predicted to rise to >700 µatm by the end of this century (IPCC, 2013), with estimates exceeding  
234 1000 µatm (Matear and Lenton, 2018; Raupach et al., 2007; Raven et al., 2005). With increasing  
235 atmospheric CO<sub>2</sub>, the oceans continue to absorb CO<sub>2</sub> from the atmosphere, which results in a  
236 shift in oceanic carbonate chemistry resulting in a decrease in seawater pH or 'Ocean  
237 Acidification' (OA). The projected increase in atmospheric CO<sub>2</sub> and corresponding increase in  
238 ocean uptake, is predicted to result in a decrease in global mean surface seawater pH of 0.3  
239 units below the present value of 8.1 to 7.8 (Wolf-gladrow et al., 1999). Under this scenario, the

240 shift in dissolved inorganic carbon (DIC) equilibria has wide ranging implications for  
241 phytoplankton photosynthetic carbon fixation rates and growth (Riebesell, 2004).

242 Concurrent with OA, elevated atmospheric CO<sub>2</sub> and other climate active gases have warmed the  
243 planet by ~0.6 °C over the past 100 years (IPCC, 2007). Atmospheric temperature has been  
244 predicted to rise by a further 1.8 to 4 °C by the end of this century (Alley et al., 2007).

245 Phytoplankton metabolic activity may be accelerated by increased temperature (Eppley, 1972),  
246 which can vary depending on the phytoplankton species and their physiological  
247 requirements (Beardall. et al., 2009; Boyd et al., 2013). Long-term data sets already suggest that  
248 ongoing changes in coastal phytoplankton communities are likely due to climate shifts and other  
249 anthropogenic influences (Edwards et al., 2006; Smetacek and Cloern, 2008; Widdicombe et al.,  
250 2010). The response to OA and temperature can potentially alter the community composition,  
251 community biomass and photo-physiology. Understanding how these two factors may interact,  
252 synergistically or antagonistically, is critical to our understanding and for predicting future  
253 primary productivity (Boyd and Doney, 2002; Dunne, 2014).

254 Laboratory studies of phytoplankton species in culture and studies on natural populations in  
255 the field have shown that most species exhibit sensitivity, in terms of growth and  
256 photosynthetic rates, to elevated pCO<sub>2</sub> and temperature individually. To date, only a few studies  
257 have investigated the interactive effects of these two parameters on natural populations (e.g.  
258 Coello-Camba et al., 2014; Feng et al., 2009; Gao et al., 2017; Hare et al., 2007). Most laboratory  
259 studies demonstrate variable results with species-specific responses. In the diatom  
260 *Thalassiosira weissflogii* for example, pCO<sub>2</sub> elevated to 1000 µatm and + 5 °C temperature  
261 synergistically enhanced growth, while the same conditions resulted in a reduction in growth  
262 for the diatom *Dactyliosolen fragilissimus* (Taucher et al., 2015). Although there have been fewer  
263 studies on dinoflagellates, variable responses have also been reported (Errera et al., 2014; Fu et  
264 al., 2008). In natural populations, elevated pCO<sub>2</sub> has stimulated the growth of pico- and  
265 nanophytoplankton (Boras et al., 2016; Engel et al., 2008) while increased temperature has  
266 reduced their biomass (Moustaka-Gouni et al., 2016; Peter and Sommer, 2012). In a recent field  
267 study on natural phytoplankton communities, elevated temperature (+ 3°C above ambient)  
268 enhanced community biomass but the combined influence of elevated temperature and pCO<sub>2</sub>  
269 reduced the biomass (Gao et al., 2017).

270 Phytoplankton species composition, abundance and biomass has been measured since 1992 at  
271 the time-series station L4 in the western English Channel (WEC), to evaluate how global  
272 changes could drive future shifts in phytoplankton community structure and carbon  
273 biogeochemistry. At this station, sea surface temperature and pCO<sub>2</sub> reach maximum values  
274 during late summer and start to decline in autumn. During October, mean seawater

275 temperatures at 10 m decrease from 15.39 °C ( $\pm$  0.49 sd) to 14.37 °C ( $\pm$  0.62 sd). Following a  
276 period of CO<sub>2</sub> oversaturation in late summer, pCO<sub>2</sub> returns to near-equilibrium at station L4 in  
277 October when mean pCO<sub>2</sub> values decrease from 455.32  $\mu$ atm ( $\pm$  63.92 sd) to 404.06  $\mu$ atm ( $\pm$   
278 38.55 sd) (Kitidis et al., 2012).

279 From a biological perspective, the autumn period at station L4 is characterised by the decline of  
280 the late summer diatom and dinoflagellate blooms (Widdicombe et al., 2010) when their  
281 biomass approaches values close to the time series minima (diatom biomass range: 6.01 ( $\pm$  6.88  
282 sd) – 2.85 ( $\pm$  3.28 sd) mg C m<sup>-3</sup>; dinoflagellate biomass range: 1.75 ( $\pm$  3.28 sd) – 0.66 ( $\pm$  1.08 sd)  
283 mg C m<sup>-3</sup>). Typically, over this period nanophytoplankton becomes numerically dominant and  
284 biomass ranges from 20.94 ( $\pm$  33.25 sd) – 9.38 ( $\pm$  3.31 sd) mg C m<sup>-3</sup>, though there is  
285 considerable variability in this biomass.

286 Based on the existing literature, the working hypotheses of this study are that: (1) community  
287 biomass will increase differentially under individual treatments of elevated temperature and  
288 pCO<sub>2</sub>; (2) elevated pCO<sub>2</sub> will lead to taxonomic shifts due to differences in species-specific CO<sub>2</sub>  
289 concentrating mechanisms and/or RuBisCO specificity; (3) photosynthetic carbon fixation rates  
290 will increase differentially under individual treatments of elevated temperature and pCO<sub>2</sub>; (4)  
291 elevated temperature will lead to taxonomic shifts due to species-specific thermal optima; (5)  
292 temperature and pCO<sub>2</sub> elevated simultaneously will have synergistic effects.

293 The objective of the study was therefore to investigate the combined effects of elevated pCO<sub>2</sub>  
294 and temperature on phytoplankton community structure, biomass and photosynthetic carbon  
295 fixation rates during the autumn transition from diatoms and dinoflagellates to  
296 nanophytoplankton at station L4 in the WEC.

## 297 **2. Materials and methods**

### 298 **2.1 Perturbation experiment, sampling and experimental set-up**

299 Experimental seawater containing a natural phytoplankton community was sampled at station  
300 L4 (50 ° 15' N, 4 ° 13' W) on 7<sup>th</sup> October 2015 from 10 m depth (40 L). The experimental  
301 seawater was gently pre-filtered through a 200  $\mu$ m Nitex mesh to remove mesozooplankton  
302 grazers, into two 20 L acid-cleaned carboys. While grazers play an important role in regulating  
303 phytoplankton community structure (e.g. Strom, 2002), our experimental goals considered only  
304 the effects of elevated temperature and pCO<sub>2</sub>, though the mesh size used does not remove  
305 microzooplankton. In addition, 320 L of seawater was collected into sixteen 20 L acid-cleaned  
306 carboys from the same depth for use as experimental media. Immediately upon return to the  
307 laboratory the media seawater was filtered through an in-line 0.2 and 0.1  $\mu$ m filter (Acropak™,



308 Pall Life Sciences) then stored in the dark at 14 °C until use. The experimental seawater was  
309 gently and thoroughly mixed and transferred in equal parts from each carboy (to ensure  
310 homogeneity) to sixteen 2.5 L borosilicate incubation bottles (4 sets of 4 replicates). The  
311 remaining experimental seawater was sampled for initial (T0) concentrations of nutrients, Chl  
312 *a*, total alkalinity, dissolved inorganic carbon, particulate organic carbon (POC) and nitrogen  
313 (PON) and was also used to characterise the starting experimental phytoplankton community.  
314 The incubation bottles were placed in an outdoor simulated in-situ incubation culture system  
315 and each set of replicates was linked to one of four 22 L reservoirs filled with the filtered  
316 seawater media. Neutral density spectrally corrected blue filters (Lee Filter no. 061) were  
317 placed between polycarbonate sheets and mounted to the top, sides and ends of the incubation  
318 system to provide ~50 % irradiance, approximating PAR measured at 10 m depth at station L4  
319 on the day of sampling prior to starting experimental incubations (see **Fig. S1**, supplementary  
320 material for time course of PAR levels during the experiment). The media was aerated with CO<sub>2</sub>  
321 free air and 5 % CO<sub>2</sub> in air precisely mixed using a mass flow controller (Bronkhorst UK  
322 Limited) and used for the microcosm dilutions as per the following experimental design: (1)  
323 control (390 µatm pCO<sub>2</sub>, 14.5 °C matching station L4 in-situ values), (2) high temperature (390  
324 µatm pCO<sub>2</sub>, 18.5 °C), (3) high pCO<sub>2</sub> (800 µatm pCO<sub>2</sub>, 14.5 °C) and (4) combination (800 µatm  
325 pCO<sub>2</sub>, 18.5 °C).

326 Initial nutrient concentrations (0.24 µM nitrate + nitrite, 0.086 µM phosphate and 2.14 µM  
327 silicate on 7<sup>th</sup> October 2015) were amended to 8 µM nitrate+nitrite and 0.5 µM phosphate.  
328 Pulses of nutrient inputs frequently occur at station L4 from August to December following  
329 heavy rainfall events and subsequent riverine inputs to the system (e.g. Barnes et al., 2015). Our  
330 nutrient amendments simulated these in situ conditions and were held constant to maintain  
331 phytoplankton growth. Previous pilot studies highlighted that if these concentrations were not  
332 maintained, the phytoplankton population crashes (Keys, 2017). As the phytoplankton  
333 community was sampled over the transitional phase from diatoms and dinoflagellates to  
334 nanophytoplankton, the in situ silicate concentration was maintained to reproduce the silicate  
335 concentrations typical of this time of year (Smyth et al., 2010). Nutrient concentrations were  
336 measured at time point T0 only.

337 Media transfer and sample acquisition was driven by peristaltic pumps. Following 48 hrs  
338 acclimation in batch culture, semi-continuous daily dilution rates were maintained at between  
339 10-13 % of the incubation bottle volume throughout the experiment. CO<sub>2</sub> enriched seawater  
340 was added to the high CO<sub>2</sub> treatment replicates every 24 hrs, acclimating the natural  
341 phytoplankton population to increments of elevated pCO<sub>2</sub> from ambient to ~800 µatm over 8  
342 days followed by maintenance at ~800 µatm as per the method described by Schulz *et al*,

343 (2009). Adding CO<sub>2</sub> enriched seawater is the preferred protocol, since some phytoplankton  
344 species are inhibited by the mechanical effects of direct bubbling (Riebesell et al., 2010; Shi et  
345 al., 2009) which causes a reduction in growth rates and the formation of aggregates (Love et al.,  
346 2016). pH was monitored daily to adjust the pCO<sub>2</sub> of the experimental media (+/-) prior to  
347 dilutions to maintain target pCO<sub>2</sub> levels in the incubation bottles. The seasonality in pH and total  
348 alkalinity (TA) are fairly stable at station L4 with high pH and low dissolved inorganic carbon  
349 (DIC) during early summer, and low pH, high DIC throughout autumn and winter (Kitidis et al.,  
350 2012). By maintaining the carbonate chemistry over the duration of the experiment, we aimed  
351 to simulate natural events at the study site.

352 To provide sufficient time for changes in the phytoplankton community to occur and to achieve  
353 an ecologically relevant data set, the incubation period was extended well beyond short-term  
354 acclimation. Previous pilot studies using the same experimental protocols highlighted that after  
355 ~20 days of incubation, significant changes in community structure and biomass were observed  
356 (Keys, 2017). These results were used to inform a more relevant incubation period of 30+ days.

## 357 **2.2 Analytical methods, experimental seawater**

### 358 **2.2.1 Chlorophyll *a***

359 Chl *a* was measured in each incubation bottle. 100 mL triplicate samples from each replicate  
360 were filtered onto 25 mm GF/F filters (nominal pore size 0.7 µm), extracted in 90 % acetone  
361 overnight at -20 °C and Chl *a* concentration was measured on a Turner Trilogy™ fluorometer  
362 using the non-acidified method of Welschmeyer (1994). The fluorometer was calibrated against  
363 a stock Chl *a* standard (*Anacystis nidulans*, Sigma Aldrich, UK), the concentration of which was  
364 determined with a Perkin Elmer™ spectrophotometer at wavelengths 663.89 and 750.11 nm.  
365 Samples for Chl *a* analysis were taken every 2-3 days.

### 366 **2.2.2 Carbonate system**

367 70 mL samples for total alkalinity (TA) and dissolved inorganic carbon (DIC) analysis were  
368 collected from each experimental replicate, stored in amber borosilicate bottles with no head  
369 space and fixed with 40 µL of super-saturated Hg<sub>2</sub>Cl<sub>2</sub> solution for later determination (Apollo  
370 SciTech™ Alkalinity Titrator AS-ALK2; Apollo SciTech™ AS-C3 DIC analyser, with analytical  
371 precision of 3 µmol kg<sup>-1</sup>). Duplicate measurements were made for TA and triplicate  
372 measurements for DIC. Carbonate system parameter values for media and treatment samples  
373 were calculated from TA and DIC measurements using the programme CO<sub>2</sub>sys (Pierrot et al.,  
374 2006) with dissociation constants of carbonic acid of Mehrbach *et al.*, (1973) refitted by Dickson

375 and Millero (Dickson and Millero, 1987). Samples for TA and DIC were taken for analysis every  
376 2-3 days throughout the experiment.

### 377 **2.2.3 Phytoplankton community analysis**

378 Phytoplankton community analysis was performed by flow cytometry (Becton Dickinson Accuri  
379 <sup>™</sup> C6) for the 0.2 to 18 µm size fraction following Tarran *et al.*, (2006) and inverted light  
380 microscopy was used to enumerate cells > 18 µm (BS EN 15204,2006). For flow cytometry, 2  
381 mL samples fixed with glutaraldehyde to a final concentration of 2 % were flash frozen in liquid  
382 nitrogen and stored at -80 °C for subsequent analysis. Phytoplankton data acquisition was  
383 triggered on both chlorophyll fluorescence and forward light scatter (FSC) using prior  
384 knowledge of the position of *Synechococcus* sp. to set the lower limit of analysis. Density plots of  
385 FSC vs. CHL fluorescence, phycoerythrin fluorescence vs. CHL fluorescence and side scatter  
386 (SSC) vs. CHL fluorescence were used to discriminate *Synechococcus* sp., picoeukaryote  
387 phytoplankton (approx. 0.5–3 µm), coccolithophores, cryptophytes, *Phaeocystis* sp. single cells  
388 and nanophytoplankton (eukaryotes >3 µm, excluding the coccolithophores, cryptophytes and  
389 *Phaeocystis* sp. single cells), [\(for further information on flow cytometer calibration for  
390 phytoplankton size measurements, see supplementary material\)](#). For inverted light microscopy,  
391 140 mL samples were fixed with 2 % (final concentration) acid Lugol's iodine solution and  
392 analysed by inverted light microscopy (Olympus<sup>™</sup> IMT-2) using the Utermöhl counting  
393 technique (Utermöhl, 1958; Widdicombe *et al.*, 2010). Phytoplankton community samples were  
394 taken at T0, T10, T17, T24 and T36.

### 395 **2.2.4 Phytoplankton community biomass**

396 The smaller size fraction identified and enumerated through flow cytometry;  
397 picophytoplankton, nanophytoplankton, *Synechococcus*, coccolithophores and cryptophytes  
398 were converted to carbon biomass (mg C m<sup>-3</sup>) using a spherical model to calculate mean cell  
399 volume:

$$400 \left(\frac{4}{3} * \pi * r^3\right) \quad \text{Equation 1.}$$

401 and a conversion factor of 0.22 pg C µm<sup>-3</sup> (Booth, 1988). A conversion factor of 0.285 pg C µm<sup>-3</sup>  
402 was used for coccolithophores (Tarran *et al.*, 2006) and cell a volume of 113 µm<sup>3</sup> and carbon  
403 cell<sup>-1</sup> value of 18 pg applied for *Phaeocystis* spp. (Widdicombe *et al.*, 2010). *Phaeocystis* spp.  
404 were identified and enumerated by flow cytometry separately to the nanophytoplankton class  
405 due to high observed abundance in in the high pCO<sub>2</sub> treatment. Mean cell measurements of  
406 individual species/taxa were used to calculate cell bio-volume for the 18 µm + size fraction

407 according to Kovalala and Larrance (1966) and converted to biomass according to the equations  
408 of Menden-Deuer & Lessard, (2000).

#### 409 **2.2.5 POC and PON**

410 Samples for particulate organic carbon (POC) and particulate organic nitrogen (PON) were  
411 taken at T0, T15 and T36. 150 mL samples were taken from each replicate and filtered under  
412 gentle vacuum pressure onto pre-ashed 25mm glass fibre filters (GF/F, nominal pore size 0.7  
413  $\mu\text{m}$ ). Filters were stored in acid washed petri-slides at  $-20\text{ }^{\circ}\text{C}$  until further processing. Sample  
414 analysis was conducted using a Thermoquest Elemental Analyser (Flash 1112). Acetanilide  
415 standards (Sigma Aldrich, UK) were used to calibrate measurements of carbon and nitrogen and  
416 also used during the analysis to account for possible drift in measured concentrations.

#### 417 **2.2.6 Chl fluorescence-based photophysiology**

418 Photosystem II (PSII) variable chlorophyll fluorescence parameters were measured using a fast  
419 repetition rate fluorometer (FRRf) (FastOcean sensor in combination with an Act2Run  
420 laboratory system, Chelsea Technologies, West Molesey, UK). The excitation wavelengths of the  
421 FRRf's light emitting diodes (LEDs) were 450, 530 and 624 nm. The instrument was used in  
422 single turnover mode with a saturation phase comprising 100 flashlets on a  $2\text{ }\mu\text{s}$  pitch and a  
423 relaxation phase comprising 40 flashlets on a  $50\text{ }\mu\text{s}$  pitch. Measurements were conducted in a  
424 temperature-controlled chamber at  $15\text{ }^{\circ}\text{C}$ . The minimum ( $F_o$ ) and maximum ( $F_m$ ) Chl  
425 fluorescence were estimated according to Kolber et al., (1998). Maximum quantum yields of PSII  
426 were calculated as:

$$427 \quad F_v / F_m = (F_m - F_o) / F_m \quad \text{Equation 2.}$$

428 PSII electron flux was calculated on a volume basis ( $JV_{\text{PSII}}$ ;  $\text{mol e}^- \text{m}^{-3} \text{d}^{-1}$ ) using the absorption  
429 algorithm (Oxborough et al., 2012) following spectral correction by normalising the FRRf LED  
430 emission to the white spectra using Fast<sup>PRO</sup> 8 software. This step required inputting the  
431 experimental phytoplankton community fluorescence excitation spectra values (FES). Since we  
432 did not measure the FES of our experimental samples, we used mean literature values for each  
433 phytoplankton group calculated proportionally (based on percentage contribution to total  
434 estimated biomass per phytoplankton group) as representative values for our experimental  
435 samples. The  $JV_{\text{PSII}}$  rates were converted to chlorophyll specific carbon fixation rates ( $\text{mg C (mg}$   
436  $\text{Chl } a)^{-1} \text{m}^{-3} \text{h}^{-1}$ ), calculated as:

$$437 \quad JV_{\text{PSII}} \times \varphi_{\text{E:C}} \times MW_{\text{C}} / \text{Chl } a \quad \text{Equation 3}$$

438 where  $\varphi_{\text{E:C}}$  is the electron requirement for carbon uptake ( $\text{molecule CO}_2 \text{ (mol electrons)}^{-1}$ ),  $MW_{\text{C}}$   
439 is the molecular weight of carbon and Chl  $a$  is the Chl  $a$  measurement specific to each sample.

440 Chl *a* specific  $JV_{PSII}$  based photosynthesis-irradiance curves were conducted in replicate batches  
441 between 10:00 – 16:00 to account for variability over the photo-period at between 8 - 14  
442 irradiance intensities. The maximum intensity applied was adjusted according to ambient  
443 natural irradiance on the day of sampling. Maximum photosynthetic rates of carbon fixation  
444 ( $P^B_m$ ), the light limited slope ( $\alpha^B$ ) and the light saturation point of photosynthesis ( $I_k$ ) were  
445 estimated by fitting the data to the model of Webb et al., (1974):

$$446 \quad P^B = (1 - e^{-\alpha \times I / P^B_m}) \quad \text{Equation 4}$$

447 Due to instrument failure during the experiment, samples for FRRf fluorescence-based light  
448 curves were taken at T36 only.

### 449 **2.3 Statistical analysis**

450 To test for effects of temperature, pCO<sub>2</sub> and possible time dependence of the measured response  
451 variables (Chl *a*, total biomass, POC, PON, photosynthetic parameters and biomass of individual  
452 species), generalized linear mixed models with the factors pCO<sub>2</sub>, temperature and time (and all  
453 interactions) were applied to the data between T0 and T36. Analyses were conducted using the  
454 lme4 package in R (R Core Team (2014). R Foundation for Statistical Computing, Vienna,  
455 Austria).

## 456 **3. Results**

457 Chl *a* concentration in the WEC at station L4 from 30 September - 6<sup>th</sup> October 2015 (when sea  
458 water was collected for the experiment) varied between 0.02-5 mg m<sup>-3</sup>, with a mean  
459 concentration of ~1.6 mg m<sup>-3</sup> (**Fig. 1 A**). Over the period leading up to phytoplankton  
460 community sampling, increasing nitrate and silicate concentrations coincided with a Chl *a* peak  
461 on 23<sup>rd</sup> September (**Fig. 1 B**). Routine net trawl (20  $\mu$ m) sample observations indicated a  
462 phytoplankton community dominated by the diatoms *Leptocylindrus danicus* and *L. minimus*  
463 with a lower presence of the dinoflagellates *Prorocentrum cordatum*, *Heterocapsa* spp. and  
464 *Oxytoxum gracile*. Following decreasing nitrate concentrations, there was a *P. cordatum* bloom  
465 on 29<sup>th</sup> September, during the week before the experiment started (data not shown).

### 466 **3.1 Experimental carbonate system**

467 Equilibration to the target high pCO<sub>2</sub> values (800  $\mu$ atm) within the high pCO<sub>2</sub> and combination  
468 treatments was achieved at T10 (**Fig. 2 A & B**). These treatments were slowly acclimated to  
469 increasing levels of pCO<sub>2</sub> over 7 days (from the initial dilution at T3) while the control and high  
470 temperature treatments were acclimated at the same ambient carbonate system values as those  
471 measured at station L4 on the day of sampling. Following equilibration, the mean pCO<sub>2</sub> values  
472 within the control and high temperature treatments were 394.9 ( $\pm$  4.3 sd) and 393.2 ( $\pm$  4.8 sd)

473  $\mu\text{atm}$  respectively, while in the high  $\text{pCO}_2$  and combination treatments mean  $\text{pCO}_2$  values were  
474  $822.6 (\pm 9.4)$  and  $836.5 (\pm 15.6 \text{ sd}) \mu\text{atm}$ , respectively. Carbonate system values remained stable  
475 throughout the experiment (For full carbonate system measured and calculated parameters, see  
476 **Table S1** in supplementary material).

### 477 **3.2 Experimental temperature treatments**

478 Mean temperatures in the control and high  $\text{pCO}_2$  treatments were  $14.1 (\pm 0.35 \text{ sd}) ^\circ\text{C}$  and in the  
479 high temperature and combination treatments the mean temperatures were  $18.6 (\pm 0.42 \text{ sd}) ^\circ\text{C}$ ,  
480 with a mean temperature difference between the ambient and high temperature treatments of  
481  $4.46 (\pm 0.42 \text{ sd}) ^\circ\text{C}$  (Supplementary material, **Fig. S2 A & B**).

482

### 483 **3.3 Chlorophyll *a***

484 Mean Chl *a* in the experimental seawater at T0 was  $1.64 (\pm 0.02 \text{ sd}) \text{ mg m}^{-3}$  (**Fig. 3 A**). This  
485 decreased in all treatments between T0 to T7, to  $\sim 0.1 (\pm 0.09, 0.035 \text{ and } 0.035 \text{ sd}) \text{ mg m}^{-3}$  in the  
486 control, high  $\text{pCO}_2$  and combination treatments, while in the high temperature treatment at T7  
487 Chl *a* was  $0.46 \text{ mg m}^{-3} (\pm 0.29 \text{ sd})$  ( $z = 2.176, p < 0.05$ ). From T7 to T12 Chl *a* increased in all  
488 treatments which was highest in the combination ( $4.99 \text{ mg m}^{-3} \pm 0.69 \text{ sd}$ ) and high  $\text{pCO}_2$   
489 treatments ( $3.83 \text{ mg m}^{-3} \pm 0.43 \text{ sd}$ ). Overall, Chl *a* was significantly influenced by experimental  
490 time, independent of experimental treatments (**Table 1**). At T36 Chl *a* concentration in the  
491 combination treatment was higher ( $6.87 (\pm 0.58 \text{ sd}) \text{ mg m}^{-3}$ ) than all other treatments while the  
492 high temperature treatment concentration was higher ( $4.77 (\pm 0.44 \text{ sd}) \text{ mg m}^{-3}$ ) than the control  
493 and high  $\text{pCO}_2$  treatment. Mean concentrations for the control and high  $\text{pCO}_2$  treatment at T36  
494 were not significantly different at  $3.30 (\pm 0.22 \text{ sd})$  and  $3.46 (\pm 0.35 \text{ sd}) \text{ mg m}^{-3}$  respectively  
495 (pairwise comparison  $t = 0.78, p = 0.858$ ).

### 496 **3.4 Phytoplankton biomass**

497 The starting biomass in all treatments was  $110.2 (\pm 5.7 \text{ sd}) \text{ mg C m}^{-3}$  (**Fig. 3 B**). The biomass was  
498 dominated by dinoflagellates ( $\sim 50\%$ ) with smaller contributions from nanophytoplankton  
499 ( $\sim 13\%$ ), cryptophytes ( $\sim 11\%$ ), diatoms ( $\sim 9\%$ ), coccolithophores ( $\sim 8\%$ ), *Synechococcus* ( $\sim 6\%$ )  
500 and picophytoplankton ( $\sim 3\%$ ). Total biomass was significantly influenced in all treatments over  
501 time (**Table 1**) and at T10, it was significantly higher in the high temperature treatment when  
502 biomass reached  $752 (\pm 106 \text{ sd}) \text{ mg C m}^{-3}$  ( $z = 2.769, p < 0.01$ ). Biomass was significantly higher  
503 in the elevated  $\text{pCO}_2$  treatment (~~and~~ interaction of time x high  $\text{pCO}_2$ ) (**Table 1**), reaching  $2481$   
504 ( $\pm 182.68 \text{ sd}$ )  $\text{mg C m}^{-3}$  at T36,  $\sim 6.5$ -fold higher than the control ~~increasing more than 20-fold~~  
505 from T0 ( $z = 3.657, p < 0.001$ ). Total biomass in the high temperature treatment at T36 was

506 significantly higher than the combination treatment and ambient control ( $z = 2.744, p < 0.001$ ),  
507 which were  $525 (\pm 28.02 \text{ sd}) \text{ mg C m}^{-3}$  and  $378 (\pm 33.95 \text{ sd}) \text{ mg C m}^{-3}$ , respectively. Reaching  
508 increased more than 15-fold to  $1735 (\pm 169.24 \text{ sd}) \text{ mg C m}^{-3}$ , at T36 biomass in the high  
509 temperature treatment was  $\sim 4.6$ -fold higher than the control, and was significantly higher than  
510 the combination treatment and ambient control ( $z = 2.744, p < 0.001$ ), which were  $525 (\pm 28.02$   
511 sd)  $\text{mg C m}^{-3}$  and  $378 (\pm 33.95 \text{ sd}) \text{ mg C m}^{-3}$ , respectively.

512 POC followed the same trends in all treatments between T0 and T36 (**Fig. 3 C**) and was in close  
513 range of the estimated biomass ( $R^2 = 0.914$ , **Fig. 3 D**). POC was significantly influenced by the  
514 interaction of time x high pCO<sub>2</sub> and time x high temperature (**Table 1**). At T36 POC was  
515 significantly higher in the high pCO<sub>2</sub> treatment ( $2086 \pm 155.19 \text{ sd mg m}^{-3}$ ) followed by the high  
516 temperature treatment ( $1594 \pm 162.24 \text{ sd mg m}^{-3}$ ),  $\sim 5.4$ -fold and 4-fold higher than the control,  
517 respectively, whereas a decline in POC was observed in the control and combination treatment.  
518 PON followed the same trend as POC over the course of the experiment, though it was only  
519 significantly influenced by the interaction between time x high pCO<sub>2</sub> (**Fig. 3 E, Table 1**). At T36  
520 concentrations were  $147 (\pm 12.99 \text{ sd})$  and  $133 (\pm 15.59 \text{ sd}) \text{ mg m}^{-3}$  in the high pCO<sub>2</sub> and high  
521 temperature treatments respectively, while PON was  $57.75 (\pm 13.07 \text{ sd}) \text{ mg m}^{-3}$  in the  
522 combination treatment and  $47.18 (\pm 9.32 \text{ sd}) \text{ mg m}^{-3}$  in the control. POC:PON ratios were  
523 significantly influenced by the interaction of time x high pCO<sub>2</sub> and time x high temperature  
524 (**Table 1**). The largest increase of 33%, from  $10.723.028 \times 10^{-5}$  to  $14.26 \text{ mg m}^{-3} 1.632 \times 10^{-4} \mu\text{M}$   
525  $\text{C}:\mu\text{M N}$  ( $\pm 1.73299 \times 10^{-5} \text{ sd}$ ) was in the high pCO<sub>2</sub> treatment (4.5-fold higher than the control at  
526 T36), followed by an increase of 32% to  $9.83 (\pm 1.82 \text{ sd}) \text{ mg m}^{-3}$  in the combination treatment  
527 (lowest T0 starting value), and an increase of 17% to  $12.091.232 \times 10^{-4} (\pm 21.1404 \times 10^{-5} \text{ sd})$   
528  $\mu\text{M C}:\mu\text{M N mg m}^{-3}$  in the high temperature treatment (3-fold higher than the control at T36).  
529 POC:PON in the combination treatment also increased over time and was 45% higher than the  
530 control at T36 ( $4.200 \times 10^{-5} \pm 5.550 \times 10^{-6} \text{ sd}$ )  $\mu\text{M C}:\mu\text{M N}$ . In contrast, the POC:PON ratio in the  
531 control declined by 20% from T0 to T36, from 10.33 to  $8.26 (\pm 0.50 \text{ sd}) \text{ mg m}^{-3}$ . (**Fig. 3 F**).

### 532 **3.5 Community composition**

533 From T0 to T24 the community shifted away from dominance of dinoflagellates in all  
534 treatments, followed by further regime shifts between T24 and T36 in the control and  
535 combination treatments. At T36 diatoms dominated the phytoplankton community biomass in  
536 the ambient control (**Fig. 4 A**), while the high temperature and high pCO<sub>2</sub> treatments exhibited  
537 near mono-specific dominance of nanophytoplankton (**Figs. 4 B & C**). The most diverse  
538 community was in the combination treatment where dinoflagellates and *Synechococcus* became  
539 more prominent (**Fig. 4 D**).

540 Between T10 and T24 the community shifted to nanophytoplankton in all experimental  
541 treatments. This dominance was maintained to T36 in the high temperature and high pCO<sub>2</sub>  
542 treatments whereas in the ambient control and combination treatment, the community shifted  
543 away from nanophytoplankton (**Fig. 5 A**). Nanophytoplankton biomass was significantly higher  
544 in the high pCO<sub>2</sub> treatment (**Table 2**) with biomass reaching 2216 ( $\pm$  189.67 sd) mg C m<sup>-3</sup> at  
545 T36. This biomass was also high (though not significantly throughout the experiment until T36)  
546 in the high temperature treatment (T36: 1489 ( $\pm$  170.32 sd) mg C m<sup>-3</sup>,  $z = 1.695$ ,  $p = 0.09$ )  
547 compared to the control and combination treatments. In the combination treatment  
548 nanophytoplankton biomass was 238 ( $\pm$  14.16 sd) mg C m<sup>-3</sup> at T36 which was higher than the  
549 control, though not significantly (162  $\pm$  20.02 sd mg C m<sup>-3</sup>). In addition to significant differences  
550 in nanophytoplankton biomass amongst the experimental treatments, treatment-specific  
551 differences in cell size were also observed. Larger nano-flagellates dominated the control (mean  
552 cell diameter of 6.34  $\mu$ m), smaller nano-flagellates dominated the high temperature and  
553 combination treatments (mean cell diameters of 3.61  $\mu$ m and 4.28  $\mu$ m) whereas *Phaeocystis* spp.  
554 dominated the high pCO<sub>2</sub> treatment (mean cell diameter 5.04  $\mu$ m) and was not observed in any  
555 other treatment (Supplementary material, **Fig. S3 A-D**).

556 At T0, diatom biomass was low and dominated by *Coscinodiscus wailessi* (48 %; 4.99 mg C m<sup>-3</sup>),  
557 *Pleurosigma* (25 %; 2.56 mg C m<sup>-3</sup>) and *Thalassiosira subtilis* (19 %; 1.94 mg C m<sup>-3</sup>). Small  
558 biomass contributions were made by *Navicula distans*, undetermined pennate diatoms and  
559 *Cylindrotheca closterium*. Biomass in the diatom group remained low from T0 to T24 but  
560 increased significantly through time in all treatments (**Table 2**), with the highest biomass in the  
561 high pCO<sub>2</sub> treatment (235  $\pm$  21.41 sd mg C m<sup>-3</sup>, **Fig. 5 B**). The highest diatom contribution to  
562 total community biomass at T36 was in the ambient control (52 % of biomass; 198  $\pm$  17.28 sd  
563 mg C m<sup>-3</sup>). In both the high temperature and combination treatments diatom biomass was lower  
564 at T36 (151  $\pm$  10.94 sd and 124  $\pm$  19.16 sd mg C m<sup>-3</sup>, respectively). In all treatments, diatom  
565 biomass shifted from the larger *C. wailessi* to the smaller *C. closterium*, *N. distans*, *T. subtilis*  
566 and *Tropidoneis* spp., the relative contributions of which were treatment-specific. Overall *N.*  
567 *distans* dominated diatom biomass in all treatments at T36 (ambient control: 112  $\pm$  24.86 sd mg  
568 C m<sup>-3</sup>, 56 % of biomass; high temperature: 106  $\pm$  17.75 sd mg C m<sup>-3</sup>, 70 % of biomass; high pCO<sub>2</sub>:  
569 152  $\pm$  19.09 sd mg C m<sup>-3</sup>, 61 % of biomass; and combination: 111  $\pm$  20.97 sd mg C m<sup>-3</sup>, 89 % of  
570 biomass; Supplementary material, **Fig. S4 A-D**).

571 The starting dinoflagellate community was dominated by *Gyrodinium spirale* (91 %; 49 mg C m<sup>-3</sup>)  
572 <sup>3</sup>), with smaller contributions from *Katodinium glaucum* (5 %; 2.76 mg C m<sup>-3</sup>), *Prorocentrum*  
573 *cordatum* (3 %; 1.78 mg C m<sup>-3</sup>) and undetermined *Gymnodiniales* (1 %; 0.49 mg C m<sup>-3</sup>). At T36  
574 Dinoflagellate biomass was significantly higher in the combination treatment (90  $\pm$  16.98 sd mg



575 C m<sup>-3</sup>, **Fig. 5 C, Table 2**) followed by the high temperature treatment (57 ± 6.87 sd mg C m<sup>-3</sup>,  
576 **Table 2**). There was no significant difference in dinoflagellate biomass between the high pCO<sub>2</sub>  
577 treatment and ambient control at T36 when biomass was low. In the combination treatment, the  
578 dinoflagellate biomass became dominated by *P. cordatum* which contributed 59 ± 12.95 sd mg C  
579 m<sup>-3</sup> (66 % of biomass in this group).

580 *Synechococcus* biomass was significantly higher in the combination treatment (reaching 59.9 ±  
581 4.30 sd mg C m<sup>-3</sup> at T36, **Fig. 5 D, Table 2**) followed by the high temperature treatment (30 ±  
582 5.98 sd mg C m<sup>-3</sup>, **Table 2**). In both the high pCO<sub>2</sub> treatment and control *Synechococcus* biomass  
583 was low (~7 mg C m<sup>-3</sup> in both treatments at T36), though an initial significant response to high  
584 pCO<sub>2</sub> was observed between T0 – T10 (**Table 2**). In all treatments and throughout the  
585 experiment, relative to the other phytoplankton groups, biomass of picophytoplankton (**Fig. 5**  
586 **E**), cryptophytes (**Fig. 5 F**) and coccolithophores (**Fig. 5 G**) remained low, though there was a  
587 slight increase in picophytoplankton in the combination treatment (11.26 ± 0.79 sd mg C m<sup>-3</sup>;  
588 **Table 2**).

589 Microzooplankton was dominated by *Strombolidium* spp. in all treatments throughout the  
590 experiment, though biomass was low relative to the phytoplankton community (**Fig. 6**).  
591 Following a decline from T0 to T10, microzooplankton biomass increased in all but the high CO<sub>2</sub>  
592 treatment until T17 when biomass diverged. The biomass trajectory maintained an increase in  
593 the control when at T36 it was highest at ~1.6 mg C m<sup>-3</sup>, 90% higher than the high temperature  
594 treatment (0.83 mg C m<sup>-3</sup>). Microzooplankton biomass was significantly lower in the high CO<sub>2</sub>  
595 treatment at T36 ( $z = -2.100, p = 0.036$ ) and undetected in the combination treatment at this  
596 time point (**Table 2**).

597

### 598 **3.6 Chl *a* fluorescence-based photophysiology**

599 At T36, FRRf photosynthesis-irradiance (PE) parameters were strongly influenced by the  
600 experimental treatments. P<sup>B</sup><sub>m</sub> was significantly higher in the high pCO<sub>2</sub> treatment (18.93 mg C  
601 (mg Chl *a*)<sup>-1</sup> m<sup>-3</sup> h<sup>-1</sup>), followed by the high temperature treatment (9.58 mg C (mg Chl *a*)<sup>-1</sup> m<sup>-3</sup> h<sup>-1</sup>;  
602 **Fig. 6Z, Tables 3 & 4**). There was no significant difference in P<sup>B</sup><sub>m</sub> between the control and  
603 combination treatments (2.77 and 3.02 mg C (mg Chl *a*)<sup>-1</sup> m<sup>-3</sup> h<sup>-1</sup>). Light limited photosynthetic  
604 efficiency (α<sup>B</sup>) also followed the same trend and was significantly higher in the high pCO<sub>2</sub>  
605 treatment (0.13 mg C (mg Chl *a*)<sup>-1</sup> m<sup>-3</sup> h<sup>-1</sup> (μmol photon m<sup>-2</sup> s<sup>-1</sup>)<sup>-1</sup>) followed by the high  
606 temperature treatment (0.09 mg C (mg Chl *a*)<sup>-1</sup> m<sup>-3</sup> h<sup>-1</sup> (μmol photon m<sup>-2</sup> s<sup>-1</sup>)<sup>-1</sup>; **Tables 3 & 4**). α<sup>B</sup>  
607 was low in both the control and combination treatment (0.03 and 0.04 mg C (mg Chl *a*)<sup>-1</sup> m<sup>-3</sup> h<sup>-1</sup>  
608 (μmol photon m<sup>-2</sup> s<sup>-1</sup>)<sup>-1</sup>, respectively). The light saturation point of photosynthesis (*E*<sub>k</sub>) was

609 significantly higher in the high pCO<sub>2</sub> treatment relative to all treatments (144.13 μmol photon  
610 m<sup>-2</sup> s<sup>-1</sup>), though significantly lower in the combination treatment relative to both the high pCO<sub>2</sub>  
611 and high temperature treatments (**Tables 3 & 4**).

#### 612 **4. Discussion**

613 Individually, elevated temperature and pCO<sub>2</sub> resulted in the highest biomass and maximum  
614 photosynthetic rates (P<sup>B<sub>m</sub></sup>) at T36, when nanophytoplankton dominated. The interaction of  
615 these two factors had little effect on total biomass with values close to the ambient control, and  
616 no effect on P<sup>B<sub>m</sub></sup>. The combination treatment, however, exhibited the greatest diversity of  
617 phytoplankton functional groups with dinoflagellates and *Synechococcus* becoming dominant  
618 over time.

619 Elevated pCO<sub>2</sub> has been shown to enhance the growth and photosynthesis of some  
620 phytoplankton species which have active uptake systems for inorganic carbon (Giordano et al.,  
621 2005; Reinfelder, 2011). Elevated pCO<sub>2</sub> may therefore lead to lowered energetic costs of carbon  
622 assimilation in some species and a redistribution of the cellular energy budget to other  
623 processes (Tortell et al., 2002). In ~~this~~the present study, under elevated pCO<sub>2</sub> where the  
624 dominant group was nanophytoplankton, ~~the community was dominated by the bloom-~~  
625 ~~forming~~the most abundant species was the haptophyte *Phaeocystis* spp. Photosynthetic carbon  
626 fixation in *Phaeocystis* spp. is presently near saturation with respect to current levels of pCO<sub>2</sub>  
627 (Rost et al., 2003). Dominance of this spp. under elevated pCO<sub>2</sub> ~~is likely~~may be ~~to be~~ due to  
628 ~~lowered grazing pressure variability in the C acquisition strategy, which could be advantageous~~  
629 ~~over other species; since microzooplankton biomass was lowest in the high CO<sub>2</sub> treatment~~  
630 ~~throughout the experiment~~. The increased biomass and photosynthetic carbon fixation in this  
631 experimental community under elevated pCO<sub>2</sub> is due to the community shift to *Phaeocystis* spp..  
632 The increased biomass in the high temperature treatment (where microzooplankton biomass  
633 remained stable between T17 to T36, though lower than the control) may be attributed to  
634 enhanced enzymatic activities, since algal growth commonly increases with temperature until  
635 after an optimal range (Boyd et al., 2013; Goldman and Carpenter, 1974; Savage et al., 2004).  
636 Optimum growth temperatures for marine phytoplankton are often several degrees higher than  
637 environmental temperatures (Eppley, 1972; Thomas et al., 2012). Nanophytoplankton also  
638 dominated in this treatment and while *Phaeocystis* spp. was not discriminated, no further  
639 classification was made at a group/species level. Reduced biomass in the control from T24  
640 onwards may be due to increased grazing pressure given the highest concentrations of  
641 microzooplankton biomass were observed in the control. Conversely, microzooplankton  
642 biomass declined significantly from T17 in the combination treatment, indicating reduced  
643 grazing pressure while phytoplankton biomass also declined from this time point. Nutrient

644 concentrations were not measured beyond T0 and we cannot therefore exclude the possibility  
645 that differences in nutrient availability may have contributed to observed differences between  
646 control and high temperature and high CO<sub>2</sub> treatments.

#### 647 **4.1 Chl *a***

648 Biomass in the control peaked at T25 followed by a decline to T36. Correlated with this, Chl *a*  
649 also peaked at T25 in the control and declined to 3.3 mg m<sup>-3</sup> by T27, remaining close to this  
650 value until T36. Biomass in the combination treatment peaked at T20 followed by decline to  
651 T36 whereas Chl *a* in this treatment declined from T20 to T25 followed by an increase at T27  
652 before further decline similar to the biomass. Chl *a* peaked in this treatment again at T36 (6.8  
653 mg m<sup>-3</sup>). We attribute the increase in Chl *a* between T25 – T27 (coincident with an overall  
654 biomass decrease) to lower species specific carbon:Chl *a* ratios as a result of the increase in  
655 dinoflagellates, *Synechococcus* and picophytoplankton biomass from T25. We speculate that  
656 the decline in biomass under nutrient replete conditions in the combination treatment was  
657 probably due to slower species-specific growth rates when diatoms and dinoflagellates  
658 dominated/became more prominent in this treatment. Carbon:Chl *a* in diatoms and  
659 dinoflagellates have previously been demonstrated to be lower than nano- and  
660 picophytoplankton (Sathyendranath et al., 2009). This contrasts the results reported in  
661 comparable studies as Chl *a* is generally highly correlated with biomass, ( e.g. Feng et al., 2009).  
662 Similar results were reported however by Hare et al., (2007) which indicates that Chl *a* may not  
663 always be a reliable proxy for biomass in mixed communities.

#### 664 **4.2 Biomass**

665 This study shows that the phytoplankton community response to elevated temperature and  
666 pCO<sub>2</sub> is highly variable. pCO<sub>2</sub> elevated to ~800 μatm induced higher community biomass, similar  
667 to the findings of Kim et al., (2006) and Riebesell et al., (2007), whereas in other natural  
668 community studies no CO<sub>2</sub> effect on biomass was observed (Delille et al., 2005; Maugendre et al.,  
669 2017; Paul et al., 2015). A ~4.5 °C increase in temperature also resulted in higher biomass at  
670 T36 in this study, similar to the findings of Feng et al., (2009) and Hare et al., (2007) though  
671 elevated temperature has previously reduced biomass of natural nanophytoplankton  
672 communities in the Western Baltic Sea and Arctic Ocean (Coello-Camba et al., 2014; Moustaka-  
673 Gouni et al., 2016). When elevated temperature and pCO<sub>2</sub> were combined, community biomass  
674 exhibited little response, similar to the findings of Gao et al., (2017), though an increase in  
675 biomass has also been reported (Calbet et al., 2014; Feng et al., 2009). Geographic location and  
676 season also play an important role in structuring the community and its response in terms of  
677 biomass to elevated temperature and pCO<sub>2</sub>. (Li et al., 2009; Morán et al., 2010). This may explain

678 part of the variability in responses observed from studies on phytoplankton during different  
679 seasons and provinces.

### 680 **4.3 Carbon:Nitrogen**

681 In agreement with others, the results of this experiment showed highest increases in C:N under  
682 elevated pCO<sub>2</sub> alone (Riebesell et al., 2007). C:N also increased under high temperature,  
683 consistent with the findings of Lomas and Glibert, (1999) and Taucher et al., (2015). It also  
684 increased when pCO<sub>2</sub> and temperature were elevated, albeit to a lesser degree, which was also  
685 observed by Calbet et al., (2014), but contrasts other studies that have observed C:N being  
686 unaffected by the combined influence of elevated pCO<sub>2</sub> and temperature (Deppeler and  
687 Davidson, 2017; Kim et al., 2006; C. Paul et al., 2015). C:N is a strong indicator of cellular protein  
688 content (Woods and Harrison, 2003) and increases under elevated pCO<sub>2</sub> and warming may lead  
689 to lowered nutritional value of phytoplankton which has implications for zooplankton  
690 reproduction and the biogeochemical cycling of nutrients.

### 691 **4.4 Photosynthetic carbon fixation rates**

692 At T36, under elevated pCO<sub>2</sub> P<sup>B</sup><sub>m</sub> was > 6 times higher than in the control, but only one time  
693 point was measured so we are not able to make decisive conclusions. which has also been  
694 reported by Riebesell et al., (2007) and Tortell et al., (2008) also reported an increase in P<sup>B</sup><sub>m</sub>  
695 under elevated pCO<sub>2</sub>. By contrast other observations on natural populations under elevated  
696 pCO<sub>2</sub> reported a reduction in P<sup>B</sup><sub>m</sub> (Feng et al., 2009; Hare et al., 2007). Studies on laboratory  
697 cultures have shown that increases in temperature cause an increase photosynthetic rates  
698 (Feng et al., 2008; Fu et al., 2007; Hutchins et al., 2007), similar to what we observed in this  
699 study. In the combined pCO<sub>2</sub> and temperature treatment, we found no effect on P<sup>B</sup><sub>m</sub>, which has  
700 also been observed in experiments on natural populations (Coello-Camba and Agustí, 2016; Gao  
701 et al., 2017). This contrasts the findings of Feng et al., (2009) and Hare et al., (2007) who  
702 observed the highest P<sup>B</sup><sub>m</sub> when temperature and pCO<sub>2</sub> were elevated simultaneously. In this  
703 study, increases in α<sup>B</sup> and E<sub>k</sub> under elevated pCO<sub>2</sub>, and a decrease in these parameters when  
704 elevated pCO<sub>2</sub> and temperature were combined also contrasts the trends reported by Feng et  
705 al., (2009). We should stress however, that while our photophysiological measurements support  
706 our observed trends in community biomass, they were made on a single occasion at the end of  
707 the experiment. Future experiments should focus on acquiring photophysiological  
708 measurements throughout.

709 Species specific photosynthetic rates have been demonstrated to decrease beyond at their  
710 thermal optimum temperature of 20 °C (Raven and Geider, 1988) which can be modified  
711 through photoprotective rather than photosynthetic pigments (Kiefer and Mitchell, 1983). This

712 may explain the difference in  $P^B_m$  between the high pCO<sub>2</sub> and high temperature treatments (in  
713 addition to differences in nanophytoplankton community composition in relation to *Phaeocystis*  
714 spp. discussed above), as the experimental high temperature treatment in this study was ~4.5 °  
715 C higher than the control.

716 There was no significant effect of combined elevated pCO<sub>2</sub> and temperature on  $P^B_m$ , which was  
717 strongly influenced by taxonomic differences between the experimental treatments. Warming  
718 has been shown to lead to smaller cell sizes in nanophytoplankton (Atkinson et al., 2003; Peter  
719 and Sommer, 2012), which was observed in the combined treatment together with decreased  
720 nanophytoplankton biomass. Diatoms also shifted to smaller species with reduced biomass,  
721 while dinoflagellate and *Synechococcus* biomass increased at T36. Dinoflagellates are the only  
722 photoautotrophs with form II RuBisCO (Morse et al., 1995) which has the lowest  
723 carboxylation:oxygenation specificity factor among eukaryotic phytoplankton (Badger et al.,  
724 1998), which may give dinoflagellates a disadvantage in carbon fixation under present ambient  
725 pCO<sub>2</sub> levels. Phytoplankton growth rates are generally slower in surface waters with high pH  
726 (≥9) resulting from photosynthetic removal of CO<sub>2</sub> by previous blooms and the associated  
727 nutrient depletion, as is the case with dinoflagellates (Hansen, 2002; Hinga, 2002). Though  
728 growth under high pH provides indirect evidence that dinoflagellates possess CCMs, direct  
729 evidence is limited and points to the efficiency of CCMs in dinoflagellates as moderate in  
730 comparison to diatoms and some haptophytes (Reinfelder, 2011 and references therein). This  
731 may Given that dinoflagellates accounted for just ~20% of biomass in the combination  
732 treatment, exerting a minor influence on community photosynthetic rates, further work is  
733 required to explain the lower  $P^B_m$  in the under the combined influence of elevated pCO<sub>2</sub> and  
734 temperature combined treatment compared to the individual treatment influences elevated  
735 pCO<sub>2</sub> and temperature individually. We applied the same electron requirement parameter for  
736 carbon uptake across all treatments, though in nature and between species, there can be  
737 considerable variation in this parameter (e.g. 1.15 to 54.2 mol e<sup>-</sup> (mol C)<sup>-1</sup>; Lawrenz et al., 2013)  
738 which can co-vary with temperature, nutrients, Chl *a*, irradiance and community structure.  
739 Better measurement techniques at quantifying this variability are necessary in the future.

#### 740 **4.5 Community composition**

741 Phytoplankton community structure changes were observed, with a shift from dinoflagellates to  
742 nanophytoplankton which was most pronounced under single treatments of elevated  
743 temperature and pCO<sub>2</sub>. Amongst the nanophytoplankton, a distinct size shift to smaller cells was  
744 observed in the high temperature and combination treatments, while in the high pCO<sub>2</sub>  
745 treatment *Phaeocystis* spp. dominated. Under combined pCO<sub>2</sub> and temperature from T24  
746 onwards however, dinoflagellate and *Synechococcus* biomass increased and nanophytoplankton

747 biomass decreased. An increase in pico- and nanophytoplankton has previously been reported  
748 in natural communities under elevated pCO<sub>2</sub> (Bermúdez et al., 2016; Boras et al., 2016;  
749 Brussaard et al., 2013; Engel et al., 2008) while no effect on these size classes has been observed  
750 in other studies (Calbet et al., 2014; Paulino et al., 2007). Moustaka-Gouni et al., (2016) also  
751 found no CO<sub>2</sub> effect on natural nanophytoplankton communities but increased temperature  
752 reduced the biomass of this group. Kim et al., (2006) observed a shift from nanophytoplankton  
753 to diatoms under elevated pCO<sub>2</sub> alone while a shift from diatoms to nanophytoplankton under  
754 combined elevated pCO<sub>2</sub> and temperature has been reported (Hare et al., 2007). A variable  
755 response in *Phaeocystis* spp. to elevated pCO<sub>2</sub> has also been reported with increased growth  
756 (Chen et al., 2014; Keys et al., 2017), no effect (Thoisen et al., 2015) and decreased growth  
757 (Hoogstraten et al., 2012) observed. *Phaeocystis* spp. can outcompete other phytoplankton and  
758 form massive blooms (up to 10 g C m<sup>-3</sup>) with impacts on food webs, global biogeochemical  
759 cycles and climate regulation (Schoemann et al., 2005). While not a toxic algal species,  
760 *Phaeocystis* spp. are considered a harmful algal bloom (HAB) species when biomass reaches  
761 sufficient concentrations to cause anoxia through the production of mucus foam which can clog  
762 the feeding apparatus of zooplankton and fish (Eilertsen & Raa, 1995).

763 Recently published studies on the response of diatoms to elevated pCO<sub>2</sub> and temperature vary  
764 greatly. For example, Taucher et al., (2015) showed that *Thalassiosira weissflogii* incubated at  
765 1000 µatm pCO<sub>2</sub> increased growth by 8 % while for *Dactyliosolen fragilissimus*, growth  
766 increased by 39 %; temperature elevated by + 5°C also had a stimulating effect on *T. weissflogii*  
767 but inhibited the growth rate of *D. fragilissimus*; and when the treatments were combined  
768 growth was enhanced in *T. weissflogii* but reduced in *D. fragilissimus*. In our study, elevated pCO<sub>2</sub>  
769 increased biomass in diatoms (time dependent), but elevated temperature and the combination  
770 of these factors reduced the signal of this response. A distinct size-shift in diatom species was  
771 observed in all treatments, from the larger *Coscinodiscus* spp., *Pleurosigma* and *Thalassiosira*  
772 *subtilis* to the smaller *Navicula distans*. This was most pronounced in the combination treatment  
773 where *N. distans* formed 89 % of diatom biomass. *Navicula* spp. previously exhibited a  
774 differential response to both elevated temperature and pCO<sub>2</sub>. At + 4.5 °C and 960 ppm CO<sub>2</sub>  
775 Torstensson et al., (2012) observed no synergistic effects on the benthic *Navicula directa*.  
776 Elevated temperature increased growth rates by 43 % while a reduction of 5 % was observed  
777 under elevated CO<sub>2</sub>. No effects on growth were detected at pH ranging from 8 – 7.4 units in  
778 *Navicula* spp. (Thoisen et al., 2015), while there was a significant increase in growth in *N.*  
779 *distans* along a CO<sub>2</sub> gradient at a shallow cold-water vent system (Baragi et al., 2015).



780 *Synechococcus* grown under pCO<sub>2</sub> elevated to 750 ppm and temperature elevated by 4 °C  
781 resulted in increased growth and a 4-fold increase in P<sup>B<sub>m</sub></sup> (Fu et al., 2007) which is similar to the  
782 results of the present study.

783 The combination of elevated temperature and pCO<sub>2</sub> significantly increased dinoflagellate  
784 biomass to 17 % of total biomass. This was due to *P. cordatum* which increased biomass by  
785 more than 30-fold from T0 to T30 (66 % of dinoflagellate biomass in this treatment). Despite  
786 the global increase in the frequency of HABs few studies have focussed on the response of  
787 dinoflagellates to elevated pCO<sub>2</sub> and temperature. In laboratory studies at 1000 ppm CO<sub>2</sub>,  
788 growth rates of the HAB species *Karenia brevis* increased by 46 %, at 1000 ppm CO<sub>2</sub> and + 5 °C  
789 temperature it's growth increased by 30 % but was reduced under elevated temperature alone  
790 (Errera et al., 2014). A combined increase in pCO<sub>2</sub> and temperature enhanced both the growth  
791 and P<sup>B<sub>m</sub></sup> in the dinoflagellate *Heterosigma akashiwo*, whereas in contrast to the present findings,  
792 only pCO<sub>2</sub> alone enhanced these parameters in *P. cordatum* (Fu et al., 2008).

## 793 5. Implications

794 Increased biomass, P<sup>B<sub>m</sub></sup> and a community shift to nanophytoplankton under individual increases  
795 in temperature and pCO<sub>2</sub> suggests a potential positive/negative feedback on atmospheric CO<sub>2</sub>,  
796 whereby more CO<sub>2</sub> is removed from the ocean, and hence from the atmosphere through an  
797 increase in photosynthesis. The selection of *Phaeocystis* spp. under elevated pCO<sub>2</sub> indicates the  
798 potential for negative impacts on ecosystem function and food web structure due to the  
799 formation of hypoxic zones which can occur under eutrophication, inhibitory feeding effects and  
800 lowered fecundity in many copepods associated with this species (Schoemann et al., 2005;  
801 Verity et al., 2007). While more CO<sub>2</sub> is fixed, selection for nanophytoplankton in both of these  
802 treatments however, may result in reduced carbon sequestration due to slower sinking rates of  
803 the smaller phytoplankton cells (Bopp et al., 2001; Laws et al., 2000). When temperature and  
804 pCO<sub>2</sub> were elevated simultaneously, community biomass showed little response and no effects  
805 on P<sup>B<sub>m</sub></sup> were observed. This suggests a negative/no change on feedback onto atmospheric CO<sub>2</sub>  
806 and climate warming due to reduced drawdown of CO<sub>2</sub> in future warmer high CO<sub>2</sub> oceans.  
807 Additionally, combined elevated pCO<sub>2</sub> and temperature significantly modified taxonomic  
808 composition, by reducing diatom biomass relative to the control with an increase in  
809 dinoflagellate biomass dominated by the HAB species, *P. cordatum*. This has implications for  
810 fisheries, ecosystem function and human health.

## 811 6. Conclusion

812 These experimental results provide new evidence that increases in pCO<sub>2</sub> coupled with rising sea  
813 temperatures may have antagonistic effects on the autumn phytoplankton community in the  
814 WEC. Under future global change scenarios, the size range and biomass of diatoms may be  
815 reduced with increased dinoflagellate biomass and the selection of HAB species. The  
816 experimental simulations of year 2100 temperature and pCO<sub>2</sub> demonstrate that the effects of  
817 warming can be offset by elevated pCO<sub>2</sub>, ~~potentially reducing~~maintaining current levels of  
818 coastal phytoplankton productivity ~~and~~while significantly altering the community structure,  
819 and in turn these shifts will have consequences on carbon biogeochemical cycling in the WEC.

820 **Data availability:** Experimental data used for analysis will be made available (DOI will be  
821 created)

822 **Author contributions:** Matthew Keys collected, measured, processed and analysed the data and  
823 prepared the figures. Drs Gavin Tilstone and Helen Findlay conceived, directed and sought the  
824 necessary funds to support the research. Matthew Keys and Dr Gavin Tilstone wrote the paper  
825 with input from Claire Widdicombe and Professor Tracy Lawson. Claire Widdicombe supervised  
826 and advised on phytoplankton taxonomic classifications.

827 **Competing interests:** The authors declare that they have no conflict of interest.

828 **Acknowledgements:** G.H.T, H.S.F. and C.E.W were supported by the UK Natural Environment  
829 Research Council's (NERC) National Capability – The Western English Channel Observatory  
830 (WCO). C.E.W was also partly funded by the NERC and Department for Environment, Food and  
831 Rural Affairs, Marine Ecosystems Research Program (Grant no. NE/L003279/1). M.K. was  
832 supported by a NERC PhD studentship (grant No. NE/L50189X/1). We thank Glen Tarran for his  
833 training, help and assistance with flow cytometry, The National Earth Observation Data Archive  
834 and Analysis Service UK (NEODAAS) for providing the MODIS image used in Fig 1. and the crew  
835 of RV Plymouth Quest for their helpful assistance during field sampling.

## 836 **References**

837 Alley, D., Berntsen, T., Bindoff, N. L., Chen, Z. L., Chidthaisong, A., Friedlingstein, P., Gregory, J., G.,  
838 H., Heimann, M., Hewitson, B., Hoskins, B., Joos, F., Jouzel, Kattsov, V., Lohmann, U., Manning, M.,  
839 Matsuno, T., Molina, M., Nicholls, N., Overpeck, J., Qin, D.H., Raga, G. Ramaswamy, V., Ren, J.W.,  
840 Rusticucci, M., Solomon, S. and Somerville, R., Stocker, T.F., Stott, P., Stouffer, R.J. Whetton, P.,  
841 Wood, R.A. & Wratt, D.: Climate Change 2007. The Physical Science basis: Summary for  
842 policymakers. Contribution of Working Group I to the Fourth Assessment Report of the  
843 Intergovernmental Panel on Climate Change, in ... Climate Change 2007. The Physical Science



844 Basis, Summary for Policy Makers.... [online] Available from:  
845 <http://scholar.google.com/scholar?hl=en&btnG=Search&q=intitle:Climate+Change+2007+:+The+Physical+Science+Basis+Summary+for+Policymakers+Contribution+of+Working+Group+I+to+the+Fourth+Assessment+Report+of+the#3> (Accessed 24 October 2013), 2007.

848 Atkinson, D., Ciotti, B. J. and Montagnes, D. J. S.: Protists decrease in size linearly with  
849 temperature: ca. 2.5% C<sup>-1</sup>, *Proc. R. Soc. B Biol. Sci.*, 270(1533), 2605–2611,  
850 doi:10.1098/rspb.2003.2538, 2003.

851 Badger, M. R., Andrews, T. J., Whitney, S. M., Ludwig, M., Yellowlees, D. C., Leggat, W. and Price, G.  
852 D.: The diversity and coevolution of Rubisco , plastids , pyrenoids , and chloroplast-based CO<sub>2</sub> -  
853 concentrating mechanisms in algae 1, *Can. J. Bot.*, (76), 1052–1071, 1998.

854 Baragi, L. V., Khandeparker, L. and Anil, A. C.: Influence of elevated temperature and pCO<sub>2</sub> on the  
855 marine periphytic diatom *Navicula distans* and its associated organisms in culture,  
856 *Hydrobiologia*, 762(1), 127–142, doi:10.1007/s10750-015-2343-9, 2015.

857 Barnes, M. K., Tilstone, G. H., Smyth, T. J., Widdicombe, C. E., Gloël, J., Robinson, C., Kaiser, J. and  
858 Suggett, D. J.: Drivers and effects of *Karenia mikimotoi* blooms in the western English Channel,  
859 *Prog. Oceanogr.*, 137, 456–469, doi:10.1016/j.pcean.2015.04.018, 2015.

860 Beardall, J., Stojkovic, S. and Larsen, S.: Living in a high CO<sub>2</sub> world: impacts of global climate  
861 change on marine phytoplankton, *Plant Ecol. Divers.*, 2(2), 191–205,  
862 doi:10.1080/17550870903271363, 2009.

863 Bermúdez, J. R., Riebesell, U., Larsen, A. and Winder, M.: Ocean acidification reduces transfer of  
864 essential biomolecules in a natural plankton community, *Sci. Rep.*, 6(1), 27749,  
865 doi:10.1038/srep27749, 2016.

866 Booth, B. C.: Size classes and major taxonomic groups of phytoplankton at two locations in the  
867 subarctic pacific ocean in May and August, 1984, *Mar. Biol.*, 97(2), 275–286,  
868 doi:10.1007/BF00391313, 1988.

869 Bopp, L. , Monfray, P. , Aumont, O. , Dufresne, J.-L. , Le Treut, H. , Madec, G. , Terray, L. . and  
870 Orr, J. C. .: Potential impact of climate change on marine export production, *Global Biogeochem.*  
871 *Cycles*, 15(1), 81–99, doi:10.1029/1999GB001256, 2001.

872 Boras, J. A., Borrull, E., Cardelu, C., Cros, L., Gomes, A., Sala, M. M., Aparicio, F. L., Balague, V.,  
873 Mestre, M., Movilla, J., Sarmiento, H., Va, E. and Lo, A.: Contrasting effects of ocean acidification on  
874 the microbial food web under different trophic conditions, *ICES J. Mar. Sci.*, 73(73 (3)), 670–679,  
875 2016.

876 Boyd, P. W. and Doney, S. C.: Modelling regional responses by marine pelagic ecosystems to  
877 global climate change, *Geophys. Res. Lett.*, 29(16), 1–4, 2002.

878 Boyd, P. W., Rynearson, T. A., Armstrong, E. A., Fu, F., Hayashi, K., Hu, Z., Hutchins, D. A., Kudela,  
879 R. M., Litchman, E., Mulholland, M. R., Passow, U., Strzepek, R. F., Whittaker, K. A., Yu, E. and  
880 Thomas, M. K.: Marine Phytoplankton Temperature versus Growth Responses from Polar to  
881 Tropical Waters - Outcome of a Scientific Community-Wide Study, *PLoS One*, 8(5),  
882 doi:10.1371/journal.pone.0063091, 2013.

883 Brussaard, C. P. D., Noordeloos, A. A. M., Witte, H., Collenteur, M. C. J., Schulz, K., Ludwig, A. and  
884 Riebesell, U.: Arctic microbial community dynamics influenced by elevated CO<sub>2</sub> levels,  
885 *Biogeosciences*, 10(2), 719–731, doi:10.5194/bg-10-719-2013, 2013.

886 Calbet, A., Sazhin, A. F., Nejstgaard, J. C., Berger, S. a, Tait, Z. S., Olmos, L., Sousoni, D., Isari, S.,  
887 Martínez, R. a, Bouquet, J.-M., Thompson, E. M., Båmstedt, U. and Jakobsen, H. H.: Future climate  
888 scenarios for a coastal productive planktonic food web resulting in microplankton phenology  
889 changes and decreased trophic transfer efficiency., *PLoS One*, 9(4), e94388,  
890 doi:10.1371/journal.pone.0094388, 2014.

891 Chen, S., Beardall, J. and Gao, K.: A red tide alga grown under ocean acidification upregulates its  
892 tolerance to lower pH by increasing its photophysiological functions, *Biogeosciences*, 11, 4829–  
893 4837, doi:10.5194/bg-11-4829-2014, 2014.

894 Coello-Camba, A. and Agustí, S.: Acidification counteracts negative effects of warming on diatom  
895 silicification, *Biogeosciences Discuss.*, 30(October), 1–19, doi:10.5194/bg-2016-424, 2016.

896 Coello-Camba, A., Agustí, S., Holding, J., Arrieta, J. M. and Duarte, C. M.: Interactive effect of  
897 temperature and CO<sub>2</sub> increase in Arctic phytoplankton, *Front. Mar. Sci.*,  
898 1(October), 1–10, doi:10.3389/fmars.2014.00049, 2014.

899 Delille, B., Harlay, J., Zondervan, I., Jacquet, S., Chou, L., Wollast, R., Bellerby, R. G. J.,  
900 Frankignoulle, M., Borges, A. V., Riebesell, U. and Gattuso, J.-P.: Response of primary production  
901 and calcification to changes of p CO<sub>2</sub> during experimental blooms of the coccolithophorid  
902 *Emiliana huxleyi*, *Global Biogeochem. Cycles*, 19(2), n/a-n/a, doi:10.1029/2004GB002318,  
903 2005.

904 Deppeler, S. L. and Davidson, A. T.: Southern Ocean Phytoplankton in a Changing Climate, *Front.*  
905 *Mar. Sci.*, 4(February), doi:10.3389/fmars.2017.00040, 2017.

906 Dickson, A. G. and Millero, F. J.: A comparison of the equilibrium constants for the dissociation of  
907 carbonic acid in seawater media, *Deep Sea Res. Part I Oceanogr. Res. Pap.*, 34(111), 1733–1743,

908 1987.

909 Dunne, J. P.: A roadmap on ecosystem change, *Nat. Clim. Chang.*, 5, 20 [online] Available from:  
910 <http://dx.doi.org/10.1038/nclimate2480>, 2014.

911 Edwards, M., Johns, D., Leterme, S. C., Svendsen, E. and Richardson, A. J.: Regional climate change  
912 and harmful algal blooms in the northeast Atlantic, *Limnol. Oceanogr.*, 51(2), 820–829,  
913 doi:10.4319/lo.2006.51.2.0820, 2006.

914 Eilertsen, H. and Raa, J.: Toxins in seawater produced by a common phytoplankter : *phaeocystis*  
915 *pouchetii*, *J. Mar. Biotechnol.*, 3(1), 115–119 [online] Available from:  
916 <http://ci.nii.ac.jp/naid/10002209414/en/> (Accessed 28 January 2016), 1995.

917 Engel, A., Schulz, K. G., Riebesell, U., Bellerby, R., Delille, B. and Schartau, M.: Effects of CO<sub>2</sub> on  
918 particle size distribution and phytoplankton abundance during a mesocosm bloom experiment  
919 (PeECE II), *Biogeosciences*, 5, 509–521, doi:10.5194/bgd-4-4101-2007, 2008.

920 Eppley, R. W.: Temperature and phytoplankton growth in the sea, *Fish. Bull.*, 70(4), 1063–1085,  
921 1972.

922 Errera, R. M., Yvon-Lewis, S., Kessler, J. D. and Campbell, L.: Responses of the dinoflagellate  
923 *Karenia brevis* to climate change: pCO<sub>2</sub> and sea surface temperatures, *Harmful Algae*, 37, 110–  
924 116, doi:10.1016/j.hal.2014.05.012, 2014.

925 Feng, Y., Warner, M. E., Zhang, Y., Sun, J., Fu, F.-X., Rose, J. M. and Hutchins, D. a.: Interactive  
926 effects of increased pCO<sub>2</sub>, temperature and irradiance on the marine coccolithophore *Emiliana*  
927 *huxleyi* (Prymnesiophyceae), *Eur. J. Phycol.*, 43(1), 87–98, doi:10.1080/09670260701664674,  
928 2008.

929 Feng, Y., Hare, C., Leblanc, K., Rose, J., Zhang, Y., DiTullio, G., Lee, P., Wilhelm, S., Rowe, J., Sun, J.,  
930 Nemcek, N., Gueguen, C., Passow, U., Benner, I., Brown, C. and Hutchins, D.: Effects of increased  
931 pCO<sub>2</sub> and temperature on the North Atlantic spring bloom. I. The phytoplankton community  
932 and biogeochemical response, *Mar. Ecol. Prog. Ser.*, 388, 13–25, doi:10.3354/meps08133, 2009.

933 Fu, F.-X., Warner, M. E., Zhang, Y., Feng, Y. and Hutchins, D. a.: Effects of Increased Temperature  
934 and Co<sub>2</sub> on Photosynthesis, Growth, and Elemental Ratios in Marine *Synechococcus* and  
935 *Prochlorococcus* (Cyanobacteria), *J. Phycol.*, 43(3), 485–496, doi:10.1111/j.1529-  
936 8817.2007.00355.x, 2007a.

937 Fu, F.-X., Warner, M. E., Zhang, Y., Feng, Y. and Hutchins, D. a.: Effects of Increased Temperature  
938 and Co<sub>2</sub> on Photosynthesis, Growth, and Elemental Ratios in Marine *Synechococcus* and  
939 *Prochlorococcus* (Cyanobacteria), *J. Phycol.*, 43(3), 485–496, doi:10.1111/j.1529-

940 8817.2007.00355.x, 2007b.

941 Fu, F.-X., Zhang, Y., Warner, M. E., Feng, Y., Sun, J. and Hutchins, D. a.: A comparison of future  
942 increased CO<sub>2</sub> and temperature effects on sympatric *Heterosigma akashiwo* and *Prorocentrum*  
943 minimum, *Harmful Algae*, 7(1), 76–90, doi:10.1016/j.hal.2007.05.006, 2008.

944 Gao, G., Jin, P., Liu, N., Li, F., Tong, S., Hutchins, D. A. and Gao, K.: The acclimation process of  
945 phytoplankton biomass, carbon fixation and respiration to the combined effects of elevated  
946 temperature and pCO<sub>2</sub> in the northern South China Sea, *Mar. Pollut. Bull.*, 118(1–2), 213–220,  
947 doi:10.1016/j.marpolbul.2017.02.063, 2017.

948 Giordano, M., Beardall, J. and Raven, J. a: CO<sub>2</sub> concentrating mechanisms in algae: mechanisms,  
949 environmental modulation, and evolution., *Annu. Rev. Plant Biol.*, 56(January), 99–131,  
950 doi:10.1146/annurev.arplant.56.032604.144052, 2005.

951 Goldman, J. and Carpenter, E.: A kinetic approach to the effect of temperature on algal growth,  
952 *Limnol. Oceanogr.*, 19(5), 756–766, doi:10.4319/lo.1974.19.5.0756, 1974.

953 Hansen, P.: Effect of high pH on the growth and survival of marine phytoplankton: implications  
954 for species succession, *Aquat. Microb. Ecol.*, 28, 279–288, doi:10.3354/ame028279, 2002.

955 Hare, C., Leblanc, K., DiTullio, G., Kudela, R., Zhang, Y., Lee, P., Riseman, S. and Hutchins, D.:  
956 Consequences of increased temperature and CO<sub>2</sub> for phytoplankton community structure in the  
957 Bering Sea, *Mar. Ecol. Prog. Ser.*, 352, 9–16, doi:10.3354/meps07182, 2007a.

958 Hare, C., Leblanc, K., DiTullio, G., Kudela, R., Zhang, Y., Lee, P., Riseman, S. and Hutchins, D.:  
959 Consequences of increased temperature and CO<sub>2</sub> for phytoplankton community structure in the  
960 Bering Sea, *Mar. Ecol. Prog. Ser.*, 352, 9–16, doi:10.3354/meps07182, 2007b.

961 Hinga, K. R.: Effects of pH on coastal marine phytoplankton, *Mar. Ecol. Prog. Ser.*, 238, 281–300,  
962 2002.

963 Hoogstraten, a., Peters, M., Timmermans, K. R. and De Baar, H. J. W.: Combined effects of  
964 inorganic carbon and light on *Phaeocystis globosa* Scherffel (Prymnesiophyceae),  
965 *Biogeosciences*, 9(5), 1885–1896, doi:10.5194/bg-9-1885-2012, 2012.

966 Hutchins, D. a., Fu, F.-X., Zhang, Y., Warner, M. E., Feng, Y., Portune, K., Bernhardt, P. W. and  
967 Mulholland, M. R.: CO<sub>2</sub> control of *Trichodesmium* N<sub>2</sub> fixation, photosynthesis, growth rates, and  
968 elemental ratios: Implications for past, present, and future ocean biogeochemistry, *Limnol.*  
969 *Oceanogr.*, 52(4), 1293–1304, doi:10.4319/lo.2007.52.4.1293, 2007.

970 Ippcc: Climate Change 2013: The Physical Science Basis. Contribution of Working Group I to the

971 Fifth Assessment Report of the Intergovernmental Panel on Climate Change, Intergov. Panel  
972 Clim. Chang. Work. Gr. I Contrib. to IPCC Fifth Assess. Rep. (AR5)(Cambridge Univ Press. New  
973 York), 1535, doi:10.1029/2000JD000115, 2013.

974 Keys, M.: "Effects of future CO<sub>2</sub> and temperature regimes on phytoplankton community  
975 composition, biomass and photosynthetic rates in the Western English Channel", PhD thesis.,  
976 University of Essex, United Kingdom., 2017.

977 Keys, M., Tilstone, G., Findlay, H. S., Widdicombe, C. E. and Lawson, T.: Effects of elevated CO<sub>2</sub> on  
978 phytoplankton community biomass and species composition during a spring *Phaeocystis* spp.  
979 bloom in the western English Channel, *Harmful Algae*, 67, 92–106,  
980 doi:10.1016/j.hal.2017.06.005, 2017.

981 Kiefer, D. a. and Mitchell, B. G.: A simple steady state description of phytoplankton growth based  
982 on absorption cross section and quantum efficiency, *Limnol. Oceanogr.*, 28(4), 770–776,  
983 doi:10.4319/lo.1983.28.4.0770, 1983.

984 Kim, J.-M., Lee, K., Shin, K., Kang, J.-H., Lee, H.-W., Kim, M., Jang, P.-G. and Jang, M.-C.: The effect of  
985 seawater CO<sub>2</sub> concentration on growth of a natural phytoplankton assemblage in a controlled  
986 mesocosm experiment, *Limnol. Oceanogr.*, 51(4), 1629–1636, doi:10.4319/lo.2006.51.4.1629,  
987 2006a.

988 Kim, J.-M., Lee, K., Shin, K., Kang, J.-H., Lee, H.-W., Kim, M., Jang, P.-G. and Jang, M.-C.: The effect of  
989 seawater CO<sub>2</sub> concentration on growth of a natural phytoplankton assemblage in a controlled  
990 mesocosm experiment, *Limnol. Oceanogr.*, 51(4), 1629–1636, doi:10.4319/lo.2006.51.4.1629,  
991 2006b.

992 Kitidis, V., Hardman-mountford, N. J., Litt, E., Brown, I., Cummings, D., Hartman, S., Hydes, D.,  
993 Fishwick, J. R., Harris, C., Martinez-vicente, V., Woodward, E. M. S. and Smyth, T. J.: Seasonal  
994 dynamics of the carbonate system in the Western English Channel, *Cont. Shelf Res.*, 42, 2–12,  
995 2012.

996 Kolber, Z. S., Prášil, O. and Falkowski, P. G.: Measurements of variable chlorophyll fluorescence  
997 using fast repetition rate techniques: Defining methodology and experimental protocols,  
998 *Biochim. Biophys. Acta - Bioenerg.*, 1367(1–3), 88–106, doi:10.1016/S0005-2728(98)00135-2,  
999 1998.

1000 Lawrenz, E., Silsbe, G., Capuzzo, E., Ylöstalo, P., Forster, R. M., Simis, S. G. H., Prášil, O.,  
1001 Kromkamp, J. C., Hickman, A. E., Moore, C. M., Forget, M. H., Geider, R. J. and Suggett, D. J.:  
1002 Predicting the Electron Requirement for Carbon Fixation in Seas and Oceans, *PLoS One*, 8(3),  
1003 doi:10.1371/journal.pone.0058137, 2013.

1004 Laws, E. A., Falkowski, P. G., Smith, W. O., Ducklow, H. W. and McCarthy, J. J.: Temperature effects  
1005 on export production in the open ocean, *Global Biogeochem. Cycles*, 14(4), 1231–1246,  
1006 doi:10.1029/1999GB001229, 2000.

1007 Li, W. K. W., McLaughlin, F. A., Lovejoy, C. and Carmack, E. C.: Smallest Algae Thrive As the Arctic  
1008 Ocean Freshens, *Science* (80-. ), 326(5952), 539–539, doi:10.1126/science.1179798, 2009.

1009 Lomas, M. W. and Glibert, P. M.: Interactions between NH<sub>4</sub><sup>+</sup> and NO<sub>3</sub><sup>-</sup> uptake and  
1010 assimilation: Comparison of diatoms and dinoflagellates at several growth temperatures, *Mar.*  
1011 *Biol.*, 133(3), 541–551, doi:10.1007/s002270050494, 1999.

1012 Love, B. A., Olson, M. B. and Wuori, T.: Technical Note: A minimally-invasive experimental  
1013 system for pCO<sub>2</sub> manipulation in plankton cultures  
1014 using passive gas exchange (Atmospheric Carbon Control Simulator), *Biogeosciences Discuss.*,  
1015 (December), 1–19, doi:10.5194/bg-2016-502, 2016.

1016 Matear, R. J. and Lenton, A.: Carbon–climate feedbacks accelerate ocean acidification,  
1017 *Biogeosciences*, 15(6), 1721–1732, doi:10.5194/bg-15-1721-2018, 2018.

1018 Maugendre, L., Gattuso, J. P., Poulton, A. J., Dellisanti, W., Gaubert, M., Guieu, C. and Gazeau, F.: No  
1019 detectable effect of ocean acidification on plankton metabolism in the NW oligotrophic  
1020 Mediterranean Sea: Results from two mesocosm studies, *Estuar. Coast. Shelf Sci.*, 186, 89–99,  
1021 doi:10.1016/j.ecss.2015.03.009, 2017.

1022 Mehrbach, C., Culberson, C. H., Hawley, J. E. and Pytkowicz, R. M.: Measurement of the Apparent  
1023 Dissociation Constants of Carbonic Acid in Seawater at Atmospheric Pressure, *Limnol.*  
1024 *Oceanogr.*, 18(1932), 897–907, 1973.

1025 Menden-Deuer, S. and Lessard, E. J.: Carbon to volume relationships for dinoflagellates, diatoms,  
1026 and other protist plankton, *Limnol. Oceanogr.*, 45(3), 569–579, doi:10.4319/lo.2000.45.3.0569,  
1027 2000.

1028 Morán, X. A. G., López-Urrutia, Á., Calvo-Díaz, A. and Li, W. K. W.: Increasing importance of small  
1029 phytoplankton in a warmer ocean, *Glob. Chang. Biol.*, 16(3), 1137–1144, doi:10.1111/j.1365-  
1030 2486.2009.01960.x, 2010.

1031 Morse, D., Salois, P., Markovic, P. and Hastings, J. W.: A nuclear-encoded form II RuBisCO in  
1032 dinoflagellates., *Science*, 268(5217), 1622–1624, doi:10.1126/science.7777861, 1995.

1033 Moustaka-Gouni, M., Kormas, K. A., Scotti, M., Vardaka, E. and Sommer, U.: Warming and  
1034 Acidification Effects on Planktonic Heterotrophic Pico- and Nanoflagellates in a Mesocosm  
1035 Experiment, *Protist*, 167(4), 389–410, doi:10.1016/j.protis.2016.06.004, 2016.

1036 Oxborough, K., Moore, C. M., Suggett, D. J., Lawson, T., Chan, H. G. and Geider, R. J.: Direct  
1037 estimation of functional PSII reaction center concentration and PSII electron flux on a volume  
1038 basis: a new approach to the analysis of Fast Repetition Rate fluorometry (FRRf) data, *Limnol.*  
1039 *Oceanogr. Methods*, 10, 142–154, doi:10.4319/lom.2012.10.142, 2012.

1040 Paul, C., Matthiessen, B. and Sommer, U.: Warming, but not enhanced CO<sub>2</sub> concentration,  
1041 quantitatively and qualitatively affects phytoplankton biomass, *Mar. Ecol. Prog. Ser.*, 528, 39–51,  
1042 doi:10.3354/meps11264, 2015.

1043 Paulino, a. I., Egge, J. K. and Larsen, a.: Effects of increased atmospheric CO<sub>2</sub> on small and  
1044 intermediate sized osmotrophs during a nutrient induced phytoplankton bloom, *Biogeosciences*  
1045 *Discuss.*, 4(6), 4173–4195, doi:10.5194/bgd-4-4173-2007, 2007.

1046 Peter, K. H. and Sommer, U.: Phytoplankton Cell Size: Intra- and Interspecific Effects of  
1047 Warming and Grazing, *PLoS One*, 7(11), doi:10.1371/journal.pone.0049632, 2012.

1048 Pierrot, D., Lewis, E. and Wallace, D. W. R.: MS Excel program developed for CO<sub>2</sub> system  
1049 calculations, ORNL/CDIAC-105a. Carbon Dioxide Inf. Anal. Center, Oak Ridge Natl. Lab. US Dep.  
1050 Energy, Oak Ridge, Tennessee, 2006.

1051 Raupach, M. R., Marland, G., Ciais, P., Le Quéré, C., Canadell, J. G., Klepper, G. and Field, C. B.:  
1052 Global and regional drivers of accelerating CO<sub>2</sub> emissions., *Proc. Natl. Acad. Sci. U. S. A.*, 104(24),  
1053 10288–93, doi:10.1073/pnas.0700609104, 2007.

1054 Raven. J., Caldeira. K., Elderfield. H., H.-G. and others: Ocean acidification due to increasing  
1055 atmospheric carbon dioxide, *R. Soc.*, (June), 2005.

1056 Raven, J. A. and Geider, R. J.: Temperature and algal growth, *New Phytol.*, 110(4), 441–461,  
1057 doi:10.1111/j.1469-8137.1988.tb00282.x, 1988.

1058 Reinfelder, J. R.: Carbon Concentrating Mechanisms in Eukaryotic Marine Phytoplankton, *Ann.*  
1059 *Rev. Mar. Sci.*, 3(1), 291–315, doi:10.1146/annurev-marine-120709-142720, 2011.

1060 Riebesell, U.: Effects of CO<sub>2</sub> Enrichment on Marine Phytoplankton, *J. Oceanogr.*, 60(4), 719–729,  
1061 doi:10.1007/s10872-004-5764-z, 2004.

1062 Riebesell, U., Schulz, K. G., Bellerby, R. G. J., Botros, M., Fritsche, P., Meyerhöfer, M., Neill, C.,  
1063 Nondal, G., Oschlies, a, Wohlers, J. and Zöllner, E.: Enhanced biological carbon consumption in a  
1064 high CO<sub>2</sub> ocean., *Nature*, 450(7169), 545–8, doi:10.1038/nature06267, 2007.

1065 Riebesell, U., Fabry, V. J., Hansson, L. and Gattuso, J.-P.: Guide to best practices for ocean  
1066 acidification, edited by L. H. and J. -P. G. L. U. Riebesell, V. J. Fabry, Publications Office Of The

1067 European Union., 2010.

1068 Rost, B., Riebesell, U., Burkhardt, S. and Su, D.: Carbon acquisition of bloom-forming marine  
1069 phytoplankton, *Limnol. Oceanogr.*, 48(1), 55–67, 2003.

1070 Sathyendranath, S., Stuart, V., Nair, A., Oka, K., Nakane, T., Bouman, H., Forget, M. H., Maass, H.  
1071 and Platt, T.: Carbon-to-chlorophyll ratio and growth rate of phytoplankton in the sea, *Mar. Ecol.  
1072 Prog. Ser.*, 383, 73–84, doi:10.3354/meps07998, 2009.

1073 Savage, V. M., Gillooly, J. F., Brown, J. H., West, G. B. and Charnov, E. L.: Effects of Body Size and  
1074 Temperature on Population Growth, *Am. Nat.*, 163(3), 429–441, doi:10.1086/381872, 2004.

1075 Schoemann, V., Becquevort, S., Stefels, J., Rousseau, V. and Lancelot, C.: Phaeocystis blooms in the  
1076 global ocean and their controlling mechanisms: a review, *J. Sea Res.*, 53(1–2), 43–66,  
1077 doi:10.1016/j.seares.2004.01.008, 2005.

1078 Schulz, K. G., Ramos, J. B., Zeebe, R. E. and Riebesell, U.: Biogeosciences CO<sub>2</sub> perturbation  
1079 experiments : similarities and differences between dissolved inorganic carbon and total  
1080 alkalinity manipulations, *Biogeosciences*, 6, 2145–2153, 2009.

1081 Shi, D., Xu, Y. and Morel, F. M. M.: Effects of the pH/*p*CO<sub>2</sub> control method on medium chemistry  
1082 and phytoplankton growth, *Biogeosciences*, 6(7), 1199–1207, doi:10.5194/bg-6-1199-2009,  
1083 2009.

1084 Smetacek, V. and Cloern, J. E.: On Phytoplankton Trends, *Science* (80-. ), 319(5868), 1346–1348  
1085 [online] Available from: <http://www.jstor.org/stable/20053523>, 2008.

1086 Smyth, T. J., Fishwick, J. R., AL-Moosawi, L., Cummings, D. G., Harris, C., Kitidis, V., Rees, A.,  
1087 Martinez-Vicente, V. and Woodward, E. M. S.: A broad spatio-temporal view of the Western  
1088 English Channel observatory, *J. Plankton Res.*, 32(5), 585–601, doi:10.1093/plankt/fbp128,  
1089 2010.

1090 Strom, S.: Novel interactions between phytoplankton and microzooplankton : their influence on  
1091 the coupling between growth and grazing rates in the sea, , 41–54, 2002.

1092 Tarran, G. a., Heywood, J. L. and Zubkov, M. V.: Latitudinal changes in the standing stocks of  
1093 nano- and picoeukaryotic phytoplankton in the Atlantic Ocean, *Deep Sea Res. Part II Top. Stud.  
1094 Oceanogr.*, 53(14–16), 1516–1529, doi:10.1016/j.dsr2.2006.05.004, 2006.

1095 Taucher, J., Jones, J., James, A., Brzezinski, M. A., Carlson, C. A., Riebesell, U. and Passow, U.:  
1096 Combined effects of CO<sub>2</sub> and temperature on carbon uptake and partitioning by the marine  
1097 diatoms *Thalassiosira weissflogii* and *Dactyliosolen fragilissimus*, *Limnol. Oceanogr.*, 60(3),



- 1098 901–919, doi:10.1002/lno.10063, 2015.
- 1099 Thoisen, C., Riisgaard, K., Lundholm, N., Nielsen, T. and Hansen, P.: Effect of acidification on an  
1100 Arctic phytoplankton community from Disko Bay, West Greenland, *Mar. Ecol. Prog. Ser.*, 520,  
1101 21–34, doi:10.3354/meps11123, 2015.
- 1102 Thomas, M. K., Kremer, C. T., Klausmeier, C. A. and Litchman, E.: A Global Pattern of Thermal  
1103 Adaptation in Marine Phytoplankton, *Science (80-. )*, 338(6110), 1085–1088,  
1104 doi:10.1126/science.1224836, 2012.
- 1105 Torstensson, A., Chierici, M. and Wulff, A.: The influence of increased temperature and carbon  
1106 dioxide levels on the benthic/sea ice diatom *Navicula directa*, *Polar Biol.*, 35(2), 205–214,  
1107 doi:10.1007/s00300-011-1056-4, 2012.
- 1108 Tortell, P., DiTullio, G., Sigman, D. and Morel, F.: CO<sub>2</sub> effects on taxonomic composition and  
1109 nutrient utilization in an Equatorial Pacific phytoplankton assemblage, *Mar. Ecol. Prog. Ser.*, 236,  
1110 37–43, doi:10.3354/meps236037, 2002.
- 1111 Tortell, P. D., Payne, C. D., Li, Y., Trimborn, S., Rost, B., Smith, W. O., Riesselman, C., Dunbar, R. B.,  
1112 Sedwick, P. and DiTullio, G. R.: CO<sub>2</sub> sensitivity of Southern Ocean phytoplankton, *Geophys. Res.*  
1113 *Let.*, 35(4), L04605, doi:10.1029/2007GL032583, 2008.
- 1114 Utermöhl, H.: Zur vervollkommnung der quantitativen phytoplankton-methodik, *Mitt. int. Ver.*  
1115 *theor. angew. Limnol.*, 9, 1–38, 1958.
- 1116 Verity, P. G., Brussaard, C. P., Nejstgaard, J. C., Van Leeuwe, M. a., Lancelot, C. and Medlin, L. K.:  
1117 Current understanding of *Phaeocystis* ecology and biogeochemistry, and perspectives for future  
1118 research, edited by M. A. van Leeuwe, J. Stefels, S. Belviso, C. Lancelot, P. G. Verity, and W. W. C.  
1119 Gieskes, Springer Netherlands., 2007.
- 1120 Webb, W. L., Newton, M. and Starr, D.: Carbon dioxide exchange of *Alnus rubra*, *Oecologia*, 17(4),  
1121 281–291, doi:10.1007/BF00345747, 1974.
- 1122 Welschmeyer: Fluorometric analysis of chlorophyll a in the presence of chlorophyll b and  
1123 pheopigments, *Limnol. Oceanogr.*, 39(8), 1985–1992, 1994.
- 1124 Widdicombe, C. E., Eloire, D., Harbour, D., Harris, R. P. and Somerfield, P. J.: Long-term  
1125 phytoplankton community dynamics in the Western English Channel, *J. Plankton Res.*, 32(5),  
1126 643–655, doi:10.1093/plankt/fbp127, 2010a.
- 1127 Widdicombe, C. E., Eloire, D., Harbour, D., Harris, R. P. and Somerfield, P. J.: Long-term  
1128 phytoplankton community dynamics in the Western English Channel, *J. Plankton Res.*, 32(5),

1129 643–655, doi:10.1093/plankt/fbp127, 2010b.

1130 Wolf-gladrow, B. D. A., Riebesell, U. L. F., Burkhardt, S. and Jelle, B.: Direct effects of CO<sub>2</sub>  
1131 concentration on growth and isotopic composition of marine plankton, *Tellus*, 51B, 461–476,  
1132 1999.

1133 Woods, H. A. and Harrison, J. F.: Temperature and the chemical composition of poikilothermic  
1134 organisms, , (Sidell 1998), 237–245, 2003.

1135

1136

1137

1138

1139

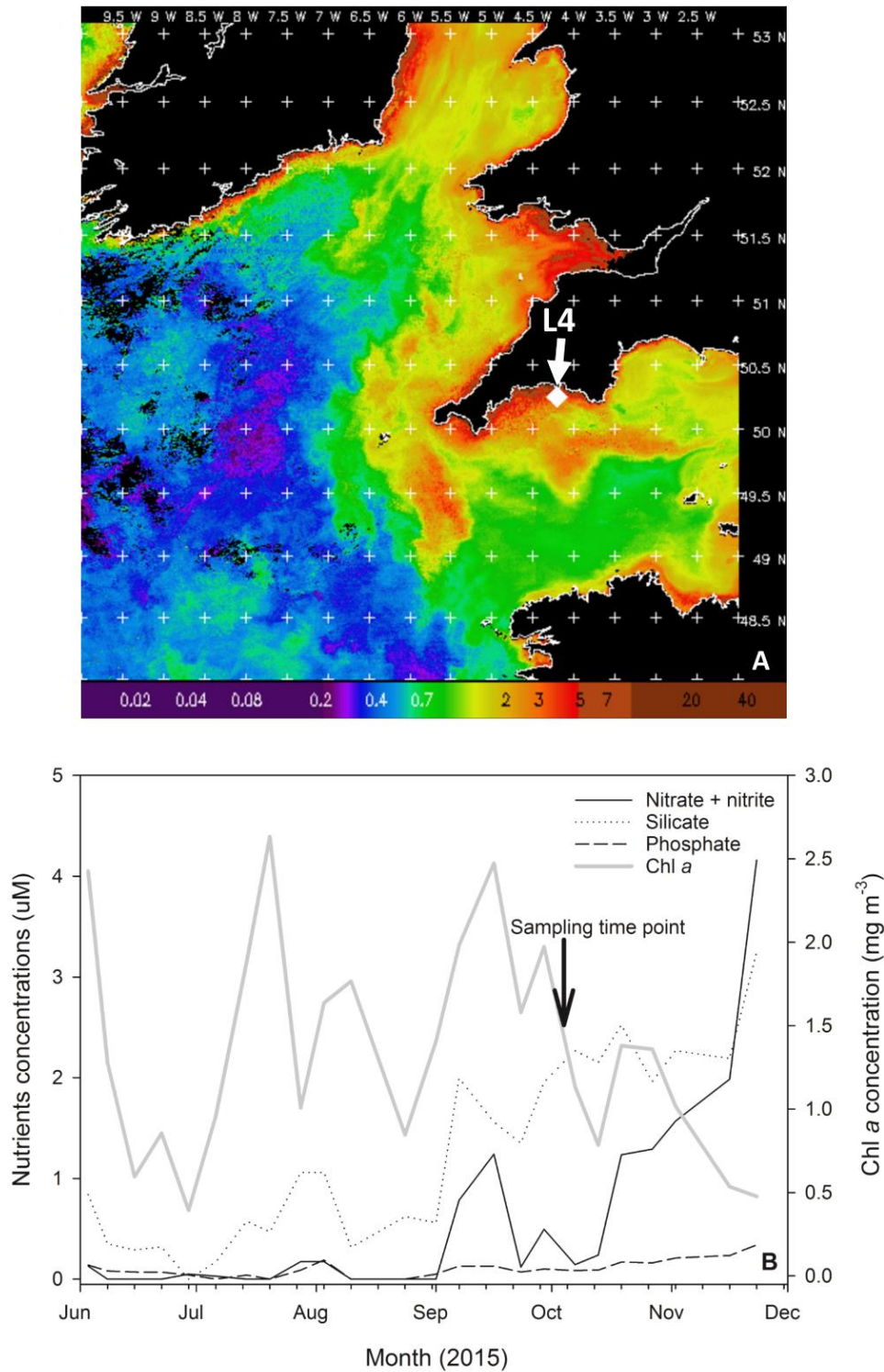


**Fig. 1.** (A). MODIS weekly composite chl *a* image of the western English Channel covering the period 30<sup>th</sup> September – 6<sup>th</sup> October 2015 (coincident with the week of phytoplankton community sampling for the present study), processing courtesy of NEODAAS. The position of coastal station L4 is marked with a white diamond. (B). Profiles of weekly nutrient and chl *a* concentrations from station L4 at a depth of 10 m over the second half of 2015 in the months prior to phytoplankton community sampling (indicated by black arrow and text).

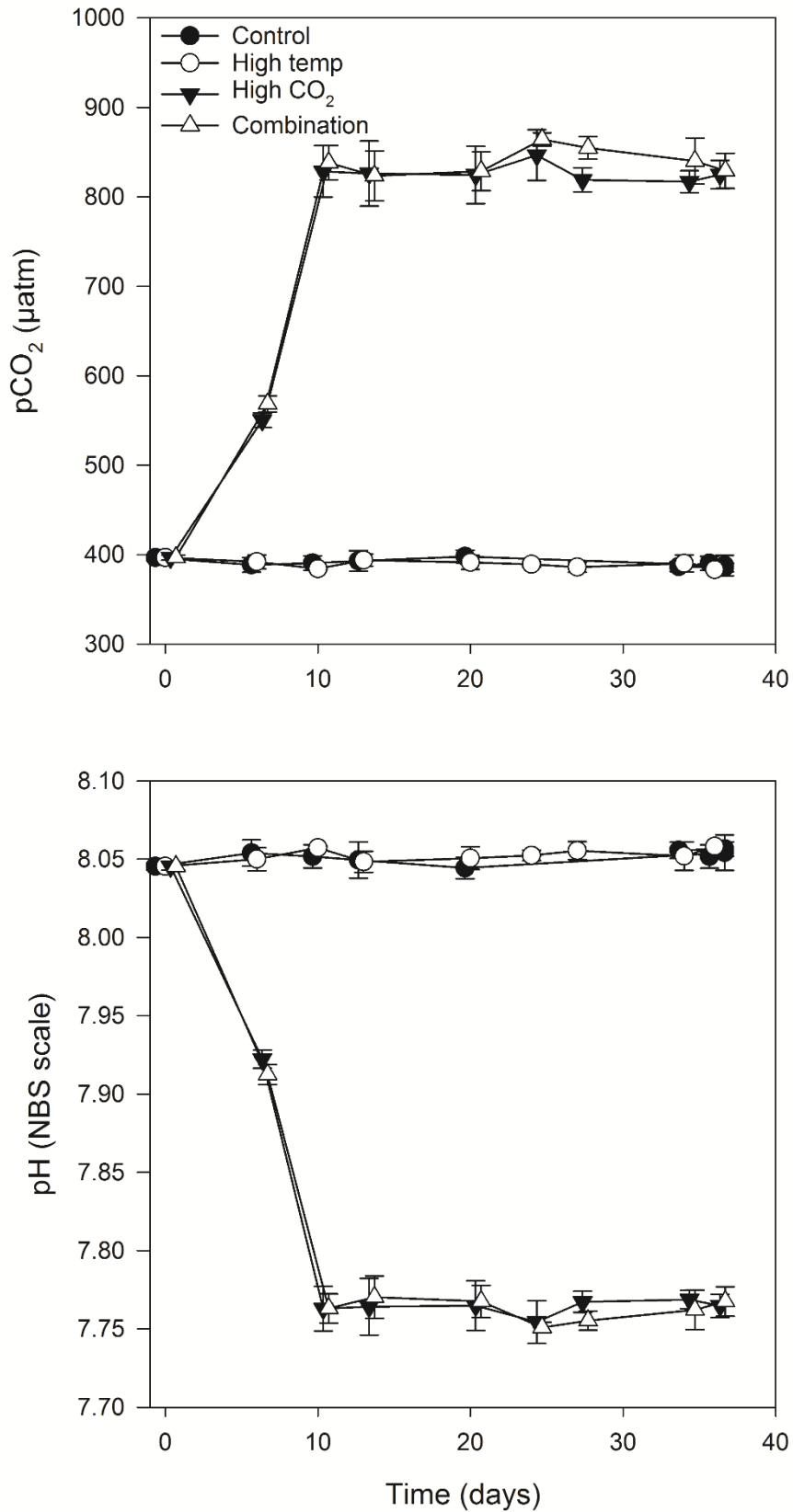


**Fig. 2.** Calculated values of partial pressure of CO<sub>2</sub> in seawater (pCO<sub>2</sub>) (A) and pH (B) from direct measurements of total alkalinity and dissolved inorganic carbon. (For full carbonate system values see **Table S1.**, supplementary material)

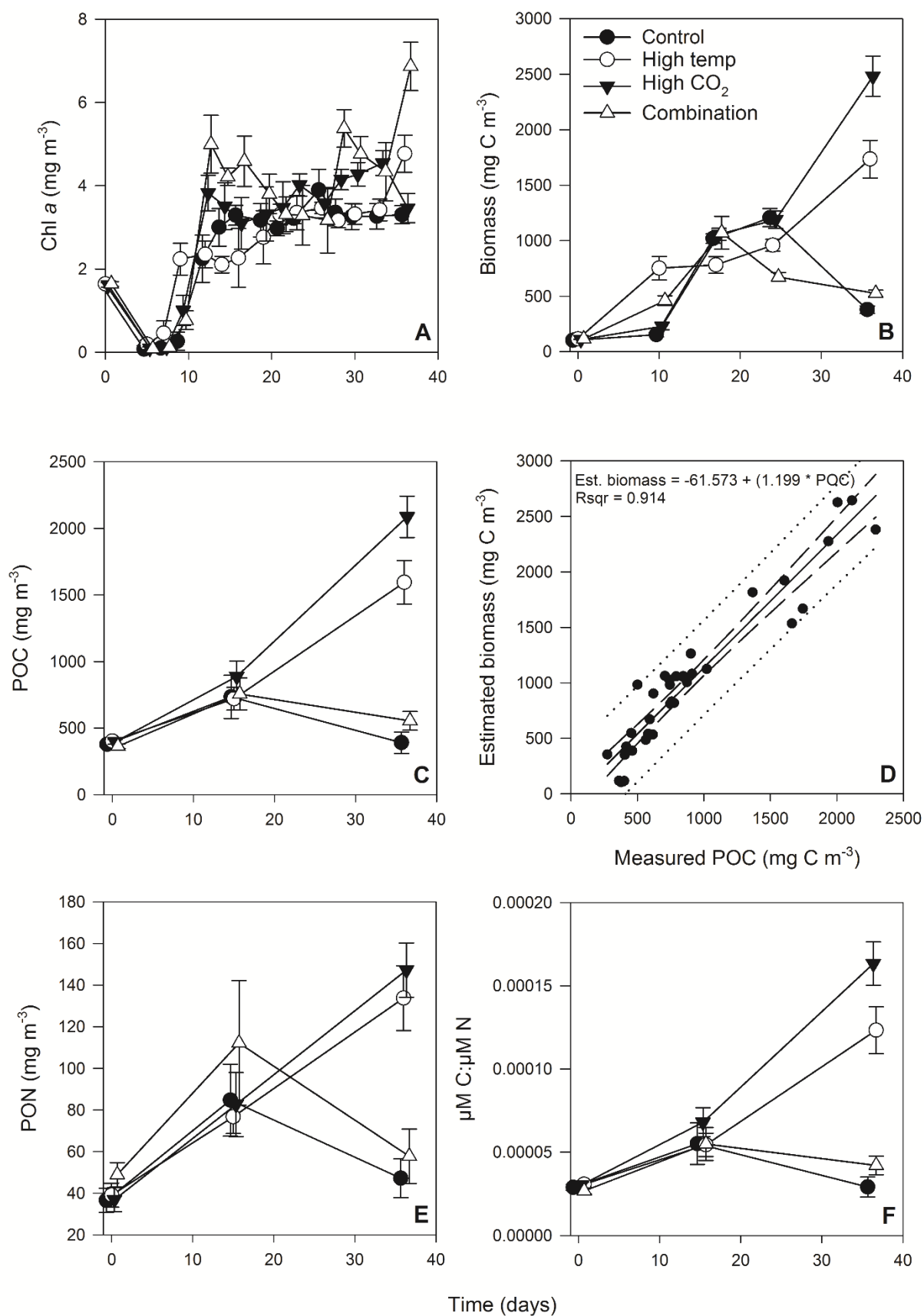


**Fig. 3.** Time course of chl *a* (A), estimated phytoplankton biomass (B), POC (C), regression of estimated phytoplankton carbon vs measured POC (D), PON (E) and POC:PON (F).

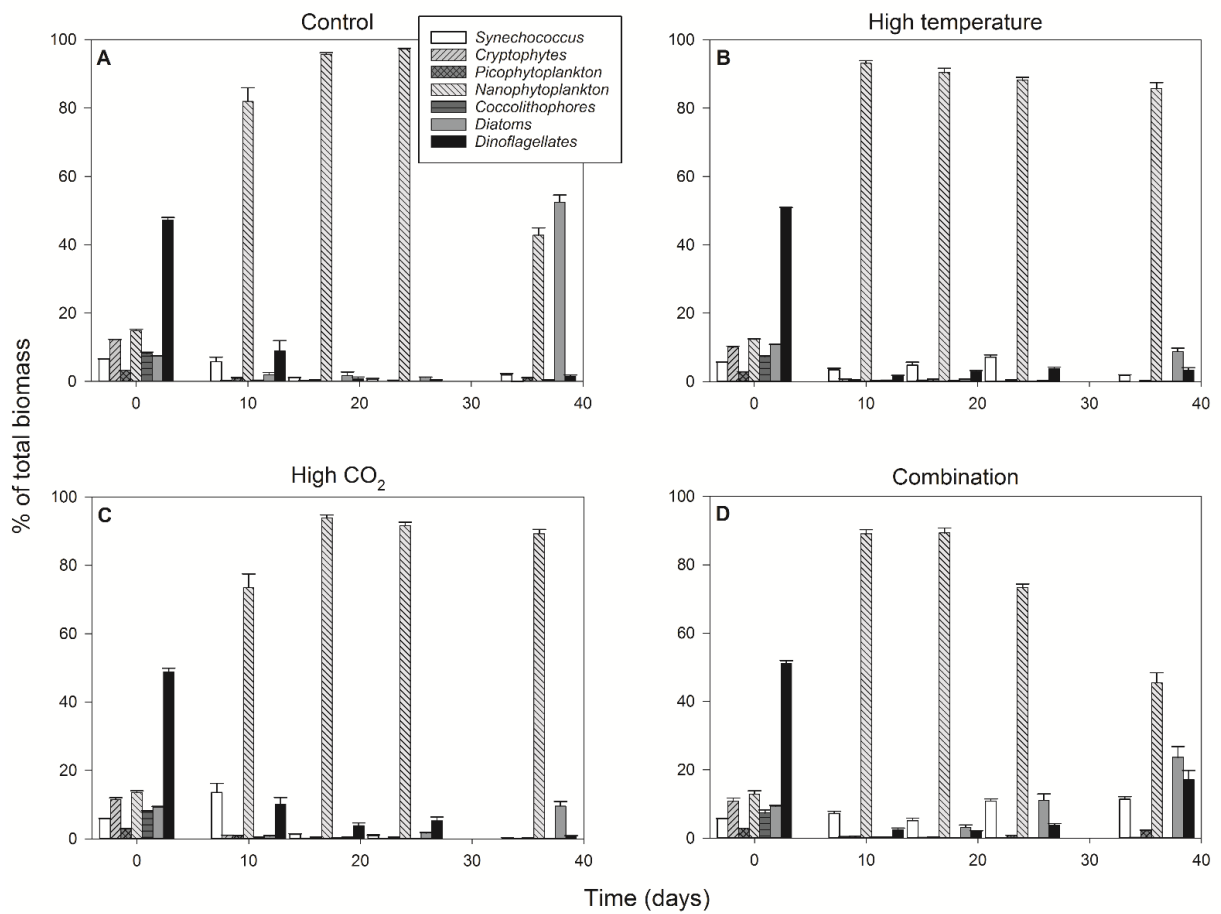


**Fig. 4.** Percentage contribution to community biomass by phytoplankton groups/species throughout the experiment in the control (A), high temperature (B), high CO<sub>2</sub> (C) and combination treatments (D).

1144

1145

1146

1147

1148

1149

1150

1151

1152

1153

1154

1155

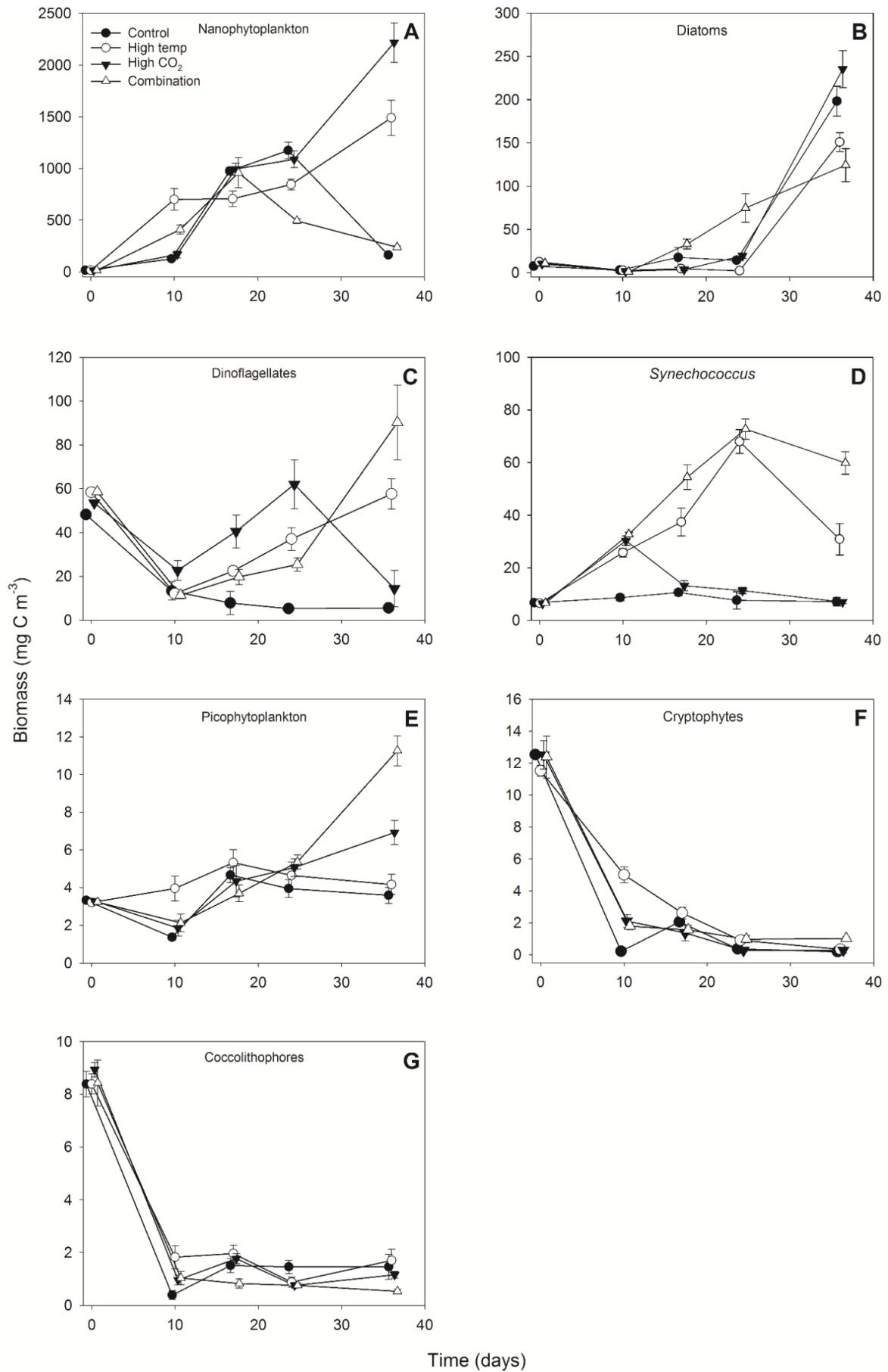


**Fig. 5.** Response of individual phytoplankton groups to experimental treatments.

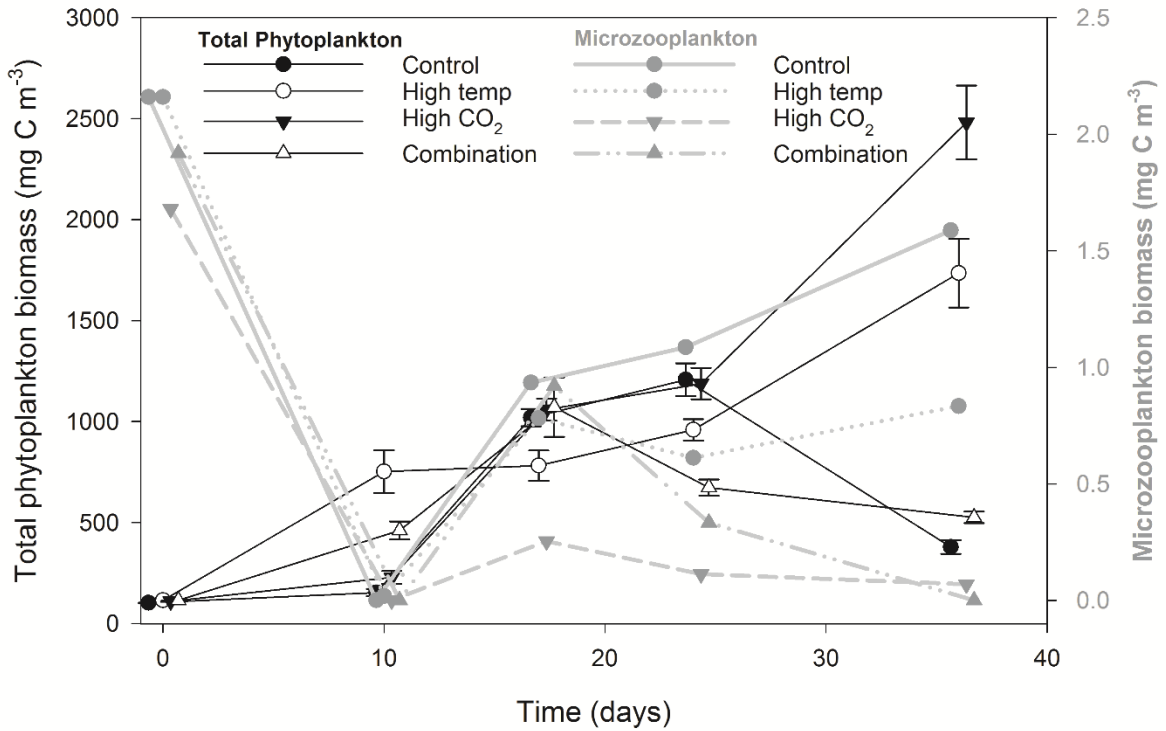


**Fig. 6.** Microzooplankton biomass (dominated by *Strombolidium* sp.) relative to total phytoplankton biomass.

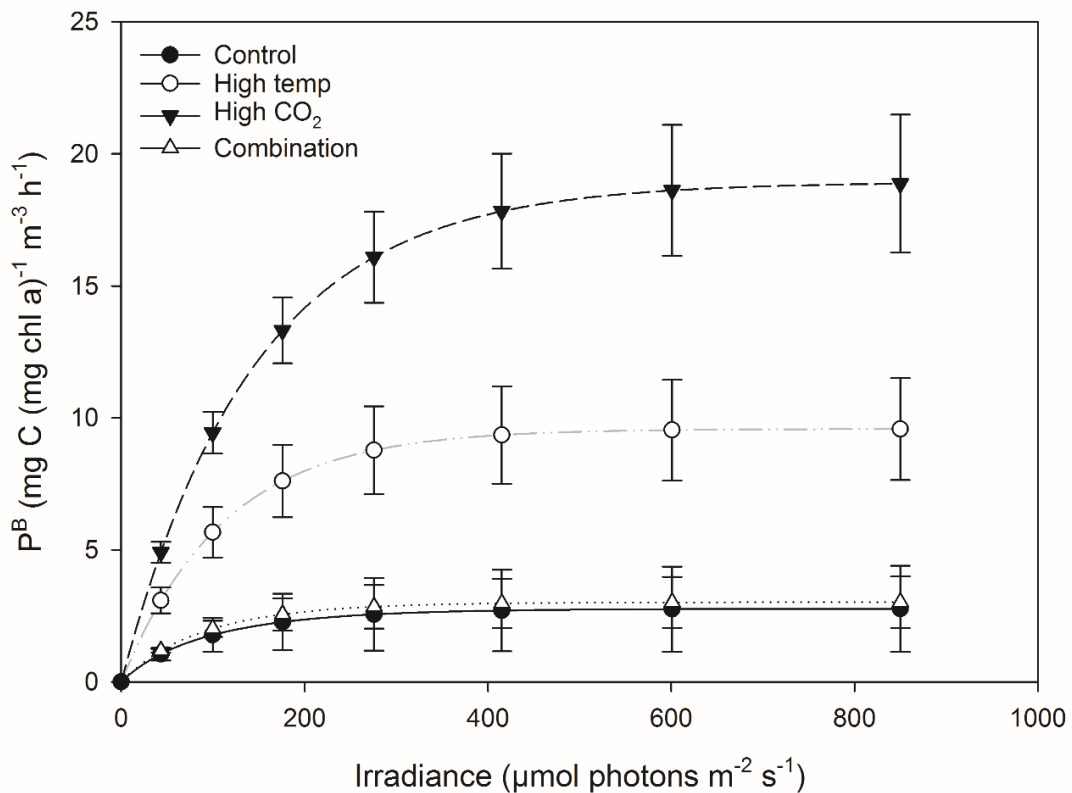


**Fig. 67.** Fitted parameters of FRRf-based photosynthesis-irradiance curves for the experimental treatments on the final experimental day (T36)



1157  
 1158  
 1159  
 1160  
 1161  
 1162  
 1163  
 1164  
 1165  
 1166  
 1167  
 1168  
 1169  
 1170

1171 **Table 1.** Results of generalized linear mixed model testing for effects of time, temperature, pCO<sub>2</sub>  
 1172 and all interactions on chl *a*, phytoplankton biomass and particulate organic carbon and  
 1173 nitrogen. Significant results are in bold; \* p < 0.05, \*\* p < 0.01, \*\*\* p < 0.001.

<b>Response variable</b>	<b>n</b>	<b>df</b>	<b>z-value</b>	<b>p</b>	<b>sig</b>
<b>Chla (mg m<sup>-3</sup>)</b>					
High temp	516	507	0.412	0.680	
High pCO <sub>2</sub>	516	507	0.664	0.507	
Time	516	507	3.815	<b>&lt;0.001</b>	<b>***</b>
High temp x high pCO <sub>2</sub>	516	507	1.100	0.271	
Time x high temp	516	507	-0.213	0.831	
Time x high CO <sub>2</sub>	516	507	-0.011	0.991	
Time x high temp x high CO <sub>2</sub>	516	507	0.340	0.734	
<b>Estimated biomass (mg C m<sup>-3</sup>)</b>					
High temp	80	71	0.092	0.927	
High pCO <sub>2</sub>	80	71	2.102	<b>0.036</b>	<b>*</b>
Time	80	71	2.524	<b>0.012</b>	<b>*</b>
High temp x high pCO <sub>2</sub>	80	71	1.253	0.210	
Time x high temp	80	71	1.866	0.062	
Time x high CO <sub>2</sub>	80	71	4.414	<b>&lt;0.001</b>	<b>***</b>
Time x high temp x high CO <sub>2</sub>	80	71	-1.050	0.294	

**POC (mg m<sup>-3</sup>)**

High temp	48	38	-0.977	0.328	
High pCO <sub>2</sub>	48	38	-0.866	0.386	
Time	48	38	-0.203	0.839	
High temp x high pCO <sub>2</sub>	48	38	-0.29	0.772	
Time x high temp	48	38	3.648	<b>&lt;0.001</b>	***
Time x high CO <sub>2</sub>	48	38	4.333	<b>&lt;0.001</b>	***
Time x high temp x high CO <sub>2</sub>	48	38	0.913	0.361	

**PON (mg m<sup>-3</sup>)**

High temp	48	38	-0.640	0.522	
High pCO <sub>2</sub>	48	38	-0.479	0.632	
Time	48	38	0.202	0.84	
High temp x high pCO <sub>2</sub>	48	38	0.667	0.505	
Time x high temp	48	38	1.674	0.094	
Time x high CO <sub>2</sub>	48	38	2.037	<b>&lt; 0.05</b>	*
Time x high temp x high CO <sub>2</sub>	48	38	-0.141	0.730	

**POC:PON  $\mu\text{M C}:\mu\text{M N}$  (mg m<sup>-3</sup>)**

High temp	48	38	<u>0.3940.222</u>	<u>0.69370.824</u>	
High pCO <sub>2</sub>	48	38	<u>0.3460.029</u>	<u>0.72950.977</u>	
Time	48	38	<u>0.1840.249</u>	<u>0.85380.803</u>	
High temp x high pCO <sub>2</sub>	48	38	<u>0.2530.990</u>	<u>0.80060.322</u>	
Time x high temp	48	38	<u>2.0352.377</u>	<b>0.04180.017</b>	*
Time x high CO <sub>2</sub>	48	38	<u>2.4452.748</u>	<b>0.01450.006</b>	**
Time x high temp x high CO <sub>2</sub>	48	38	<u>-0.673-0.215</u>	<u>0.50070.830</u>	

1174

1175 **Table 2.** Results of generalized linear mixed model testing for significant effects of time,  
 1176 temperature, pCO<sub>2</sub> and all interactions on phytoplankton species biomass. Significant results are  
 1177 in bold;

1178 \* p < 0.05, \*\* p < 0.01, \*\*\* p < 0.001.

Response variable	n	df	z-value	p	sig
<b>Diatoms (mg C m<sup>-3</sup>)</b>					
High temp	80	70	-0.216	0.829	
High pCO <sub>2</sub>	80	70	-0.895	0.371	
Time	80	70	2.951	<b>0.003</b>	**
High temp x high pCO <sub>2</sub>	80	70	1.063	0.288	
Time x high temp	80	70	-1.151	0.250	
Time x high CO <sub>2</sub>	80	70	0.560	0.576	
Time x high temp x high CO <sub>2</sub>	80	70	0.368	0.713	
<b>Dinoflagellates (mg C m<sup>-3</sup>)</b>					
High temp	80	70	-0.018	0.986	

High pCO <sub>2</sub>	80	70	0.487	0.627	
Time	80	70	-2.347	<b>0.019</b>	*
High temp x high pCO <sub>2</sub>	80	70	-0.166	0.868	
Time x high temp	80	70	1.857	0.063	
Time x high CO <sub>2</sub>	80	70	1.009	0.313	
Time x high temp x high CO <sub>2</sub>	80	70	2.207	<b>0.027</b>	*
<b>Nanophytoplankton (mg m<sup>-3</sup>)</b>					
High temp	80	70	-0.371	0.710	
High pCO <sub>2</sub>	80	70	-2.108	<b>0.035</b>	*
Time	80	70	2.162	<b>0.031</b>	*
High temp x high pCO <sub>2</sub>	80	70	0.79	0.430	
Time x high temp	80	70	1.695	0.090	
Time x high CO <sub>2</sub>	80	70	3.563	<b>&lt;0.001</b>	***
Time x high temp x high CO <sub>2</sub>	80	70	-0.806	0.420	
<b>Synechococcus (mg m<sup>-3</sup>)</b>					
High temp	80	70	3.333	<b>&lt;0.001</b>	***
High pCO <sub>2</sub>	80	70	2.231	<b>0.026</b>	*
Time	80	70	0.049	0.961	
High temp x high pCO <sub>2</sub>	80	70	2.391	<b>0.017</b>	*
Time x high temp	80	70	4.076	<b>&lt;0.001</b>	***
Time x high CO <sub>2</sub>	80	70	-1.553	0.1204	
Time x high temp x high CO <sub>2</sub>	80	70	5.382	<b>&lt;0.001</b>	***
<b>Picophytoplankton (mg m<sup>-3</sup>)</b>					
High temp	80	70	0.951	0.342	
High pCO <sub>2</sub>	80	70	-0.472	0.637	
Time	80	70	0.897	0.370	
High temp x high pCO <sub>2</sub>	80	70	-1.188	0.235	
Time x high temp	80	70	-0.219	0.827	
Time x high CO <sub>2</sub>	80	70	1.411	0.158	
Time x high temp x high CO <sub>2</sub>	80	70	2.792	<b>0.005</b>	**
<b>Coccolithophores (mg C m<sup>-3</sup>)</b>					
High temp	80	70	-0.408	0.683	
High pCO <sub>2</sub>	80	70	-0.308	0.758	
Time	80	70	0.211	0.833	
High temp x high pCO <sub>2</sub>	80	70	-0.319	0.750	
<b>Table 2 cont'd</b>					
Time x high temp	80	70	0.269	0.788	
Time x high CO <sub>2</sub>	80	70	0.295	0.768	
Time x high temp x high CO <sub>2</sub>	80	70	0.502	0.615	
<b>Cryptophytes (mg C m<sup>-3</sup>)</b>					
High temp	80	70	0.207	0.836	
High pCO <sub>2</sub>	80	70	0.256	0.798	
Time	80	70	-5.289	<b>&lt;0.001</b>	***
High temp x high pCO <sub>2</sub>	80	70	-0.349	0.727	
Time x high temp	80	70	1.885	0.059	
Time x high CO <sub>2</sub>	80	70	0.167	0.867	

Time x high temp x high CO <sub>2</sub>	80	70	1.694	0.090	
<b>Microzooplankton (mg C m<sup>-3</sup>)</b>					
High temp	80	70	0.138	0.890	
High pCO <sub>2</sub>	80	70	-0.142	0.887	
Time	80	70	0.418	0.676	
High temp x high pCO <sub>2</sub>	80	70	0.314	0.753	
Time x high temp	80	70	-0.930	0.352	
Time x high CO <sub>2</sub>	80	70	-2.100	<b>0.036</b>	*
Time x high temp x high CO <sub>2</sub>	80	70	-1.996	<b>0.046</b>	*

1179

1180

1181

1182

1183

1184

1185

1186 **Table 3.** FRRf-based photosynthesis-irradiance curve parameters for the experimental  
1187 treatments on the final day (T36).

Parameter	Control			High temp			High CO <sub>2</sub>		
	r	sd	n	r	sd	n	r	sd	n
<b>P<sup>B</sup><sub>m</sub></b>	2.77	1.63	3.02	9.58	4	18.93	2.65	3.02	0.97
<b>α</b>	0.03	0.01	0.04	0.09	1	0.13	0.01	0.04	0.00
<b>I<sub>k</sub></b>	85.33	45.4	86.38	110.93	6.0	144.13	17.9	86.38	33.0

1188

1189

1190

1191

1192

1193

1194

1195 **Table 4.** Results of generalised linear model testing for significant effects of temperature, CO<sub>2</sub>  
1196 and temperature x CO<sub>2</sub> on phytoplankton photophysiology at T36; P<sup>B</sup><sub>m</sub> (maximum  
1197 photosynthetic rates), α (light limited slope) and I<sub>k</sub> (light saturated photosynthesis). Significant  
1198 results are in bold; \* p < 0.05, \*\* p < 0.001, \*\*\* p < 0.0001.

Response variable	n	df	t-value	p	sig
-------------------	---	----	---------	---	-----

<b><u>P<sub>m</sub></u></b>					
High temp	12	8	7.353	< <b>0.0001</b>	***
High pCO <sub>2</sub>	12	8	8.735	< <b>0.0001</b>	***
High temp x high pCO <sub>2</sub>	12	8	-8.519	< <b>0.0001</b>	***
<b><u>α</u></b>					
High temp	12	8	13.03	< <b>0.0001</b>	***
High pCO <sub>2</sub>	12	8	15.15	< <b>0.0001</b>	***
High temp x high pCO <sub>2</sub>	12	8	-14.82	< <b>0.0001</b>	***
<b><u>I<sub>k</sub></u></b>					
High temp	12	8	2.018	0.0783	
High pCO <sub>2</sub>	12	8	2.541	<b>0.0347</b>	*
High temp x high pCO <sub>2</sub>	12	8	-2.441	<b>0.0405</b>	*

---

1199

1200

1201